PREPARATION AND ANTI-TUMOR ACTIVITIES ON A549 CELL LINE OF FUCOIDAN-STABILIZED GOLD NANOPARTICLES

Miss Suwicha Soisuwan

A Thesis Submitted in Partial Fulfillment of the Requirements
for the Degree of Master of Science Program in Pharmaceutical Technology
Department of Pharmaceutics and Industrial Pharmacy
Faculty of Pharmaceutical Sciences
Chulalongkorn University
Academic Year 2010

การเตรียมและฤทธิ์ต้านมะเร็งต่อเซลล์เอ 549 ของนาโนพาร์ทิเคิลทองที่เพิ่มเสถียรภาพด้วยฟูคอยแดน

นางสาวสุวิชา สร้อยสุวรรณ

วิทยานิพนธ์นี้เป็นส่วนหนึ่งของการศึกษาตามหลักสูตรปริญญาวิทยาศาสตรมหาบัณฑิต
สาขาวิชาเทคโนโลยีเภสัชกรรม ภาควิชาวิทยาการเภสัชกรรมและเภสัชอุตสาหกรรม
คณะเภสัชศาสตร์ จุฬาลงกรณ์มหาวิทยาลัย
ปีการศึกษา 2553

Thesis Title	PREPARATION AND ANTI-TUMOR ACTIVITIES ON A549 CELL LINE OF FUCOIDAN-STABILIZED GOLD NANOPARTICLES
By	Miss Suwicha Soisuwan
Field of Study	Pharmaceutical Technology
Thesis Advisor	Assistant Professor Warangkana Warisnoicharoen, Ph.D.
Thesis Co-Advisor	Kriengsak Lirdprapamongkol, Ph.D.

Accepted by the Faculty of Faculty of Pharmaceutical Sciences, Chulalongkorn University in Partial Fulfillment of the Requirements for the Master's Degree

Dean of the Faculty of
…….Pharmaceutical Sciences
(Associate Professor Pintip Pongpech, Ph.D.)

THESIS COMMITTEE

……..Chairman
(Associate Professor Parkpoom Tengamnuay, Ph.D.)

…….…….Thesis Advisor
(Assistant Professor Warangkana Warisnoicharoen, Ph.D.)

……..Thesis Co-Advisor
(Kriengsak Lirdprapamongkol, Ph.D.)

……..Examiner
(Assistant Professor Nontima Vardhanabhuti, Ph.D.)

……..External Examiner
(Ponthip Wirachwong, Ph.D.)

สุวิชา สร้อยสุวรรณ : การเตรียมและฤทธิ์ต้านมะเร็งต่อเซลล์เอ 549 ของนาโนพาร์ทิเคิลทองที่เพิ่มเสถียรภาพด้วยฟูคอยแดน. (PREPARATION AND ANTI-TUMOR ACTIVITIES ON A549 CELL LINE OF FUCOIDAN-STABILIZED GOLD NANOPARTICLES) อ. ที่ปรึกษาวิทยานิพนธ์หลัก: ผศ.ดร. วรางคณา วารีสน้อยเจริญ, อ. ที่ปรึกษาวิทยานิพนธ์ร่วม: ดร. เกรียงศักดิ์ เลิศประภามงคล, 94 หน้า.

ปัจจุบันมีการนำนาโนพาร์ทิเคิลทองมาประยุกต์ใช้ประโยชน์ในด้านต่างๆ การสังเคราะห์นาโนพาร์ทิเคิลทองด้วยสารจากธรรมชาติจึงสามารถช่วยลดการใช้สารเคมีได้ การศึกษาวิจัยนี้ได้นำสารธรรมชาติฟูคอยแดนจากสาหร่ายทะเลสีน้ำตาลสองชนิดคือ ทาคาระคอมบุ (คอมบุ) และ โอกินาวาโมซึกิ (โอกิ) มาใช้ในการเตรียมนาโนพาร์ทิเคิลทอง โดยอัตราส่วนน้ำหนักของทองต่อฟูคอยแดนที่เหมาะสมคือ 1:20 และ 1:50 สำหรับฟูคอยแดนชนิดโอกิ และคอมบุตามลำดับ และค่าเฉลี่ยเส้นผ่านศูนย์กลางของนาโนพาร์ทิเคิลทองที่ได้มีค่าเท่ากับ 8.54 ± 2.96 และ 10.74 ± 4.78 นาโนเมตร และมีขนาดประจุของอนุภาคเท่ากับ -37.77 ± 4.83 และ -21.72 ± 1.31 มิลลิโวลต์ สำหรับนาโนพาร์ทิเคิลทองที่ถูกทำให้เสถียรด้วยฟูคอยแดนชนิดโอกิและคอมบุตามลำดับ จากผลการทดลองพบว่าฟูคอยแดนชนิดโอกิสามารถเพิ่มเสถียรภาพของนาโนพาร์ทิเคิลทองได้ดีกว่าคอมบุ โดยอนุภาคทองมีการกระจายตัวของอนุภาคและมีเสถียรภาพที่ดีกว่านาโนพาร์ทิเคิลทองที่เตรียมโดยฟูคอยแดนชนิดคอมบุ ทั้งนี้อาจเนื่องจากความแตกต่างของชนิดฟูคอยแดน นอกจากนี้นาโนพาร์ทิเคิลทองที่เพิ่มเสถียรภาพด้วยฟูคอยแดนนี้ได้ถูกนำมาศึกษาฤทธิ์การต้านมะเร็งในเซลล์มะเร็งปอดของมนุษย์ (เซลล์เอ 549) จากผลการทดลองพบว่า นาโนพาร์ทิเคิลทองที่เพิ่มเสถียรภาพด้วยฟูคอยแดนมีความเป็นพิษต่อเซลล์เอ 549 มากกว่าความเป็นพิษของฟูคอยแดนอย่างเดียว และเมื่อเลี้ยงเซลล์มะเร็งในสภาพไร้การยึดเกาะพื้นผิว ก็ไม่พบการต้านทานต่อความเป็นพิษของนาโนพาร์ทิเคิลทองที่เพิ่มเสถียรภาพด้วยฟูคอยแดน ในขณะที่เซลล์มะเร็งสามารถต้านทานต่อความเป็นพิษของยาเคมีบำบัดเพิ่มขึ้น นอกจากนี้นาโนพาร์ทิเคิลทองที่เพิ่มเสถียรภาพด้วย 300 ไมโครกรัม/มิลลิลิตรของฟูคอยแดนชนิดโอกิ ยังสามารถลดการรุกรานของเซลล์มะเร็งเอ 549 (ยับยั้งการรุกรานประมาณ 16%) ซึ่งผลดังกล่าวอาจเกิดจากความสามารถในการลดการยึดเกาะของเซลล์เอ 549 กับไฟโบรเนกติน (ยับยั้งการยึดเกาะประมาณ 30%) และลดการสร้างเอนไซม์เมทริคเมททิโลโปรทิเนส-2 (ยับยั้งการสร้างเอนไซม์ประมาณ 60%) ดังนั้นนาโนพาร์ทิเคิลทองที่เพิ่มเสถียรภาพด้วยฟูคอยแดนจึงอาจสามารถนำมาประยุกต์ใช้กับการรักษาโรคมะเร็ง และควรจะมีการศึกษาถึงกลไกของนาโนพาร์ทิเคิลทองที่เพิ่มเสถียรภาพด้วยฟูคอยแดนต่อการต้านเซลล์มะเร็ง และการศึกษาในกายต่อไป

ภาควิชา วิทยาการเภสัชกรรมและเภสัชอุตสาหกรรม...ลายมือชื่อนิสิต.....

สาขาวิชา เทคโนโลยีเภสัชกรรม……...ลายมือชื่อ อ.ที่ปรึกษาวิทยานิพนธ์หลัก.....

ปีการศึกษา….2553……...ลายมือชื่อ อ.ที่ปรึกษาวิทยานิพนธ์ร่วม .....

5176859933: MAJOR PHARMACEUTICAL TECHNOLOGY

KEYWORDS : GOLD NANOPARTICLES / FUCOIDANS / ANTI-TUMOR

SUWICHA SOISUWAN: PREPARATION AND ANTI-TUMOR ACTIVITIES ON A549 CELL LINE OF FUCOIDAN-STABILIZED GOLD NANOPARTICLES. THESIS ADVISOR: ASST. PROF. WARANGKANA WARISNOICHAROEN, Ph.D., THESIS CO-ADVISOR: KRIENGSAK LIRDPRAPAMONGKOL, Ph.D., 94 pp.

Gold nanoparticles (AuNPs) are attractive to be employed in various applications. Synthesis of AuNPs using the natural substances renders benefits due to avoidance of chemical utilization. This study successfully synthesized AuNPs using natural fucoidan, Takara Kombu fucoidan (TK fucoidan) and Okinawa Mozuku fucoidan (OM fucoidan) obtained from marine brown algae. The optimum weight ratios of gold (Au) to fucoidan for preparation of AuNPs by OM fucoidan (OM-AuNPs) and TK fucoidan (TK-AuNPs) were 1:20 and 1:50, respectively. The average sizes of the obtained AuNPs were 8.54 ± 2.96 nm and 10.74 ± 4.78 nm and zeta potentials of the AuNPs were -37.77 ± 4.83 and -21.72 ± 1.31 mV, for OM-AuNPs and TK-AuNPs, respectively. According to the results, OM-AuNPs were mono-dispersed and more stable than TK-AuNPs. Hence, the difference in fucoidan type might affect the formation of AuNPs. In addition, the fucoidan-stabilized AuNPs were investigated on anti-tumor activities on A549 lung cancer cell line. The results revealed that OM-AuNPs and TK-AuNPs had a toxic effect toward cancer cells greater than the corresponding fucoidans in an anchorage-dependent condition and no sign of resistance to OM-AuNPs and TK-AuNPs was observed in an anchorage-independent condition. Likewise, OM-AuNPs containing 300 μg/ml had a slight inhibitory effect (~16% inhibition) on A549 cell invasion which might be due to an anti-adhesive effect on the cancer cells to fibronectin (~30% inhibition) and suppression of MMP-2 production of A549 cells (~60% inhibition). Conclusively, AuNPs stabilized by algal fucoidans might be promising agents for cancer treatment which should be further investigated on anti-tumor mechanisms of the AuNPs and *in vivo* study.

Department: Pharmaceutics and Industrial Pharmacy Student's Signature .....

Field of Study: Pharmceutical Technology…….. Advisor's Signature .....

Academic Year :…..2010…….. Co-Advisor's Signature .....

ACKNOWLEDGEMENTS

First of all, I would like to express thanks to Asst. Prof. Warangkana Warisnoicharoen, Ph.D. and Kriengsak Lirdprapamongkol, Ph.D. for their great suggestions, kindness and encouragement throughout my graduate study. My sincere appreciation is also to Assoc. Prof. Parkpoom Tengamnuay, Ph.D., Asst. Prof. Nontima Vardhanabhuti, Ph.D. and Ponthip Wirachwong, Ph.D. for their good discussion and participation as the thesis committee.

This study could not be completed without financial supports providing under thesis scholarship by Chulalongkorn University and Pharmaceutical Technology (International) program as well as for facilities and useful instruments to conduct the experiments.

The author would like to express gratitude to Chulabhorn Research Institute for providing useful facilities as well as all the members in the Laboratory of Biochemistry for their warmest friendship and assistance.

The author would like to thank all of the staff and members in Pharmaceutical Technology (International) Program, Faculty of Pharmaceutical Sciences, Chulalongkorn University for their kind help.

Last but not least, I would like to show sincerest and deepest appreciation to my family for their infinite love, great upbringing, understanding and encouragement throughout my life.

CONTENTS

PAGE

ABSTRACT IN THAI…… iv

ABSTRACT IN ENGLISH…… v

ACKNOWLEDGEMENTS……..……. vi

CONTENTS…… vii

LIST OF TABLES…….. x

LIST OF FIGURES…… xii

LIST OF ABBREVIATIONS…… xv

CHAPTER

I INTRODUCTION……... 1

II LITERATURE REVIEW…….. 5

1. Gold nanoparticles……...…… 5

1.1 Overview of gold nanoparticles…….. 5

1.2 Green synthesis of gold nanoparticles…… 8

1.3 Gold nanoparticles in medical areas…… 9

2. Cancer……...……... 12

2.1 Metastasis…….…… 13

2.1.1 Invasion process……..……. 14

2.1.2 Anoikis resistance……...…….. 15

3. Fucoidans……...…….. 16

3.1 Sources of fucoidans…… 17

3.2 Fucoidan structures…….…….. 17

3.3 Biological activities of fucoidans…….…… 20

3.4 Fucoidan safety …….……... 24

CHAPTER **PAGE**

III MATERIALS AND METHODS……... 25

1. Materials……...……...……... 25

1.1 Equipment…….....…….. 25

1.2 Chemicals…….……. 26

1.3 Cell lines…… 27

2. Methods…….……. 28

2.1 Preparation of AuNPs……..... 28

2.2 Characterization of fucoidan-stabilized AuNPs…… 30

2.3 Estimation of fucoidan amount in fucoidan-stabilized AuNPs……... 30

2.4 Study on anti-tumor activities of fucoidan-stabilized AuNPs……... 31

2.4.1 Preparation of samples…….…….…… 31

2.4.2 Cell cultures……..…….…… 31

2.4.3 Cytotoxic assay……...……... 32

2.4.4 Anoikis resistance assay…….……..……. 33

2.4.5 Invasion and cell migration assay……..……... 33

2.4.6 Cell adhesion assay…….……...…… 35

2.4.7 Matrix metalloproteinase-2 and -9 production assay……..... 36

2.5 Statistical analysis……..…….……... 37

IV RESULTS AND DISCUSSION…….….... 38

1. Preparation of fucoidan-stabilized gold nanoparticles……..… 38

2. Characterization of fucoidan-stabilized gold nanoparticles…. 43

3. Estimation of fucoidan amount in the colloidal gold nanoparticles……..……. 49

4. Anti-tumor tests of fucoidan-stabilized gold nanoparticles …. 50

CHAPTER **PAGE**

4.1 Cytotoxic effect of fucoidan-stabilized AuNPs on A549 cells in anchorage-independent condition……. 54

4.2 Inhibitory effect of fucoidan-stabilized AuNPs on A549 cell invasion…...……... 60

4.3 Inhibitory effect of fucoidan-stabilized AuNPs on cell migration of A549 cells……..... 62

4.4 Inhibitory effect of fucoidan-stabilized AuNPs on adhesion of A549 cells...……... 63

4.5 Inhibitory effect of fucoidan-stabilized AuNPs on matrix metalloproteinases production in A549 cells..…….. 65

V CONCLUSION…….….... 68

REFERENCES……... 70

APPENDICES……. 82

APPENDIX A: X-ray energy dispersive spectroscopy (EDS) pattern of fucodian-stabilized AuNPs…….. 83

APPENDIX B: Estimation of fucoidan amount in the colloidal gold nanoparticles…… 84

APPENDIX C: A549 cell viability after treatment with samples in anchorage-dependent condition……... 86

APPENDIX D: A549 cell viability after treatment with samples in anchorage-independent condition…… 88

APPENDIX E: Photographs of A549 cells after incubation in regular or poly-HEMA coated 96-well plate…… 90

APPENDIX F: A549 cell invasion and cell migration after 6-hour treatment with samples…… 91

APPENDIX G: A549 cell adhesion after 1-hour treatment with samples……. 92

APPENDIX H: MMP-2 production of A549 cells after 24-hour treatment with samples…… 93

VITA…… 94

LIST OF TABLES

TABLE		PAGE
1	UV peak absorption wavelength (λ_{max}) of algal fucoidan-stabilized AuNPs at various weight ratios of Au to fucoidan ……..	40
2	Zeta potential of fucoidan-stabilized AuNPs…….……	45
B1	Average concentration of OM fucoidan in the colloidal gold nanoparticles……..…….……	85
B2	Average concentration of TK fucoidan in the colloidal gold nanoparticles……..	85
B3	Fucoidan concentration in fucoidan-stabilized AuNPs colloid…….	85
C1	Percentage of viability of A549 cells after treatment with OM fucoidans and OM-AuNPs for 24 and 72 hours (Average ± S.D., n=3)…….	86
C2	Percentage of viability of A549 cells after treatment with TK fucoidans and TK-AuNPs for 24 and 72 hours (Average ± S.D., n=3)…….	86
C3	Percentage of viability of A549 cells after treatment with Cit-AuNPs for 24 and 72 hours (Average ± S.D., n=3)…….……..	87
D1	Percentage of viability of A549 cells after treatment with OM fucoidans and OM-AuNPs for 24 and 72 hours (Average ± S.D., n=3)…….	88
D2	Percentage of viability of A549 cells after treatment with TK fucoidans and TK-AuNPs for 24 and 72 hours (Average ± S.D., n=3)…….……...…….	88
D3	Percentage of viability of A549 cells after treatment with Cit-AuNPs for 24 and 72 hours (Average ± S.D., n=3)…….……..	89
F1	Percentage of invasion of A549 cells after treatment of 300 µg/ml fucoidans, fucoidan-stabilized AuNPs containing 300 µg/ml fucoidans and 215 µM Cit-AuNPs (Average ± S.D., n=3)……...……	91
F2	Percentage of cell migration of A549 cells after treatment of 300 µg/ml fucoidans, fucoidan-stabilized AuNPs containing 300 µg/ml fucoidans and 215 µM Cit-AuNPs (Average ± S.D., n=3)……..	91
G1	Percentage of adhesion of A549 cells to Matrigel® after treatment of 300 µg/ml fucoidans, fucoidan-stabilized AuNPs containing 300 µg/ml fucoidans and 215 µM Cit-AuNPs (Average ± S.D., n=3)…….	92

TABLE **PAGE**

G2 Percentage of adhesion of A549 cells to fibronectin after treatment of 300 µg/ml fucoidans, fucoidan-stabilized AuNPs containing 300 µg/ml fucoidans and 215 µM Cit-AuNPs (Average ± S.D., n=3)…….. 92

H1 Percentage of MMP-2 production of A549 cells after treatment of 300 µg/ml fucoidans, fucoidan-stabilized AuNPs containing 300 µg/ml fucoidans and 215 µM Cit-AuNPs (Average ± S.D., n=3)……. 93

LIST OF FIGURES

FIGURE		PAGE
1	Schematic of interaction of electron cloud around metal nanosphere with light…….……..	6
2	Schematic illustration for the reducing process of gold nanoparticle formation……...	8
3	Metastasic steps of cancer cells from their primary site to secondary location……..	13
4	Schematic of tumor invasion……...	15
5	Structure of algal fucoidan obtained from *C. okamuranus*……..	18
6	Three different structures of algal fucoidan obtained from *K. crassifolia*…….	19
7	Preparation of fucoidan-stabilized AuNPs…….…	29
8	Preparation of citrate-stabilized AuNPs…….…….	29
9	The schematic diagram of invasion assay……	35
10	Appearance of OM-AuNPs in varying weight ratios of Au to OM fucoidan; 1:5, 1:10, 1:20, 1:30, 1:40, 1:50 and 1:60 after synthesis (A) and one month storage (B)…….…….....	39
11	Appearance of TK-AuNPs in varying weight ratios of Au and TK fucoidan; 1:5, 1:10, 1:20, 1:30, 1:40, 1:50 and 1:60 after synthesis (A) and one month storage (B)…….……..……...	39
12	UV-Vis spectra of fucoidan-stabilized AuNPs at varying weight ratios of Au to OM fucoidan (A) and TK fucoidan (B)……	41
13	UV-Vis spectra of fucoidan-stabilized AuNPs prepared at RT; OM-AuNPs (A) and TK-AuNPs (B)……...	42
14	UV-Vis spectra of OM-AuNPs and TK-AuNPs prepared using the appropriate ratios of 1:20 and 1:50 Au to fucoidan, respectively……	43
15	UV-Vis spectra of fucoidan-stabilized AuNPs after preparation and one month storage, OM-AuNPs (ratio of 1:20) (A) and TK-AuNPs (ratio of 1:50) (B)……...…….	44

FIGURE **PAGE**

16 TEM images of OM-AuNPs after synthesis (A) and after one month storage (B). Histogram of particle size distribution of OM-AuNPs after synthesis (C) and one month storage (D)……. 47

17 TEM images of TK-AuNPs after synthesis (A) and after one month storage (B). Histogram of particle size distribution of TK-AuNPs after synthesis (C)……...……... 48

18 Percentage of viability of A549 cells after 1-day treatment with Cit-AuNPs, OM fucoidans and OM-AuNPs (A), TK fucoidan and TK-AuNPs (B) (n=3)……..……...…. 51

19 Percentage of viability of A549 cells after 3-day treatment with Cit-AuNPs, OM fucoidans and, OM-AuNPs (A) and TK fucoidan and TK-AuNPs (B) (n=3)……...…..…….. 52

20 Percentage of viability of detached A549 cells after 1-day treatment with Cit-AuNPs, OM fucoidans and OM-AuNPs (A) and TK fucoidan and TK-AuNPs (B) (n=3)……..…….. 56

21 Percentage of viability of detached A549 cells after 3-day treatment with Cit-AuNPs, OM fucoidans and OM-AuNPs (A) and TK fucoidan and TK-AuNPs (B) (n=3)…….……... 57

22 Percentage of viability of A549 cells after treatment with TK fucoidan, TK-AuNPs, OM fucoidan, OM-AuNPs (all at concentration of 300 µg/ml fucoidans), 0.1 µg/ml paclitaxel and 1 µg/ml etoposide, in anchorage-dependent and anchorage-independent conditions for one day (A) and three days (B) (n=3)……. 59

23 Percentage of invasion of A549 cells after 6-hour treatment with TK fucoidan, TK-AuNPs, OM fucoidan, OM-AuNPs (all at concentration of 300 µg/ml fucoidans) and Cit-AuNPs (n=3)……..……. 61

24 Percentage of cell migration of A549 cells (as compared to 100% of control) after 6-hour treatment with TK fucoidan, TK-AuNPs, OM fucoidan, OM-AuNPs (all at concentration of 300 µg/ml fucoidans) and Cit-AuNPs (n=3)……..……...….……...….. 63

25 Percentage of adhesion of A549 cells to Matrigel® (compared to 100% of control) after 1-hour treatment with TK fucoidan, TK-AuNPs, OM fucoidan, OM-AuNPs (all at concentration of 300 µg/ml fucoidans) and Cit-AuNPs (n=3)……...…… 64

26 Percentage of Adhesion of A549 cells to fibronectin after 1-day treatment with TK fucoidan, TK-AuNPs, OM fucoidan, OM-AuNPs (all at concentration of 300 µg/ml fucoidans) and Cit-AuNPs for six hours (n=3)…….……..... 64

FIGURE **PAGE**

27 Zymogram of fucoidan-stabilized AuNPs on MMP-2 production in A549 cells after 24-hour treatment with a control (serum-free medium), TK fucoidan, TK-AuNPs, OM fucoidan, OM-AuNPs (all at 300 µg/ml fucoidan concentration) and Cit-AuNPs (A). Effect of fucoidan-stabilized AuNPs on MMP-2 production in A549 cells after 24-hour treatment with TK fucoidan, TK-AuNPs, OM fucoidan, OM-AuNPs (all at concentration of 300 µg/ml fucoidans) and Cit-AuNPs (B)…….. 66

A1 EDS pattern of OM-AuNPs (top) and TK-AuNPs (bottom) …….. 83

B1 Examples of calibration curve between UV-absorbance and concentration of OM fucoidan (A) and TK fucoidan (B)…… 84

E1 Photographs (original magnification was x100) of A549 cells after incubation in regular 96-well plate (top) and poly-HEMA 96-well plate (bottom)……. 90

LIST OF ABBREVIATIONS

°C	degree Celsius
µg	Microgram
µl	Microliter
µM	Micromolar
A	Absorbance
ATCC	American Type Culture Collection
AuNPs	Gold nanoparticles
bFGF	Basic fibroblast growth factor
BM	Basement membrane
DDS	Drug delivery system
DMSO	Dimethylsulfoxide
ECM	Extracellular matrix
EDS	X-ray Energy Dispersive Spectroscopy
EGF	Epidermal growth factor
EGFR	Epidermal growth factor receptor
ERK	Extracellular signal-regulated kinase
EPR	Enhanced permeability and retention
et al.	*et alii* (and others)
etc.	*et cetera* (and other similar things)
FGF	Fibroblast growth factor
HBV	Hepatitis B virus
HDF-f	Human dermal fibroblasts-fetal

HGF	Hepatocyte growth factor
hr	Hour
HSV	Herpes simplex virus
IFN	Interferon
IL	Interleukin
kg	Kilogram
LPS	Lipopolysaccharide
MDR	Multi-drugs resistance
mg	Milligram
min	Minute
ml	Milliliter
mM	Millimolar
MMP	Matrix metalloproteinase
mV	Millivolt
NIR	Near infrared
nm	Nanometer
OM	Okinawa Mozuku
PBS	Phosphate buffered solution
RME	Receptor-mediated endocytosis
rpm	Round per minute
RT	Room temperature
S.D.	Standard deviation
SDS	Sodium dodecyl sulfate

SPR	Surface plasmon resonance
TEM	Transmission Electron Microscope
TGF	Transforming growth factor
TK	Takara Kombu
UV	Ultraviolet
UV-Vis	Ultraviolet-Visible
VEGF	Vascular endothelial growth factor
VEGFR	Vascular endothelial growth factor receptor
w/w	Weight by weight
WHO	World Health Organization

CHAPTER I

INTRODUCTION

1. Background and significance of the study

Nanotechnology is an innovation of tiny particles (1-100 nm in size range) which have long been rapidly developed for a decade and applied in numerous fields of technology such as electronics, communications, energy, chemistry and also in medical applications. Nanotechnology has many advantages on medical application such as imaging, diagnosis, drug delivery, tissue regeneration and drug development (Sanvicens and Marco, 2008). Nanoparticulate drug carriers which are currently developed include liposome, micelles, dendrimers, carbon nanotubes, quantum dots, protein nanoparticles, viral nanoparticles and metallic nanoparticles (Byrne, Betancourt and Brannon-Peppas, 2008). These formulations can be tailored to provide more specificity of drug delivery to target sites in order to increase efficacy and safety for patients.

Gold nanoparticles (AuNPs) are one kind of metallic nanoparticles which have many applications in medical areas such as biosensing, bioimaging and drug delivery system. The advantages of AuNPs include less toxicity and biocompatibility. Their small sizes are able to easily reach the sites of action, preventing the degradation process by an immune system. In addition, the synthesized processes of AuNPs provide strong binding toward thiol, disulfide and amine groups of compounds. Interestingly, unique optical properties of AuNPs involving surface plasmon resonance of electron clouds around metal atoms depend on size and shape of the nanoparticles (Ghosh *et al.*, 2008).

Since, AuNPs have been applied in many kinds of field, an eco-friendly synthesized method of the nanoparticles are concerned. The benefits of an eco-friendly method are to reduce of chemical substances involving in process and to eliminate the toxic wastes thus increasing safety for the community (Sun *et al.*, 2008). There are some recent reports on green synthesis of metallic nanoparticles by using biopolymers such as chitosan (Huang and Yang, 2004), dextran (Nath *et al.*, 2008) and other natural materials including marine alga (Singaravelu *et al.*, 2007) and fungus (Bhainsa and D'Souza, 2006).

Cancer is a serious disease in which abnormal cells divide uncontrollably and are able to spread across other organs. These abnormal cells are capable to establish in many organs such as skin, breast, and gastro-intestinal organs. Lung cancer is one of the most common causes of death in patients worldwide. At present, major therapeutic problems of cancer are metastasis, multi-drugs resistance (MDR) and severe side effects from conventional therapy (World Health Organization [WHO], 2009). Therefore, natural substances are considerate to be an alternative way for cancer treatment.

Fucoidans are natural sulphated polysaccharides extracted from marine brown algae and some marine invertebrates. Algal fucoidans are widely found in several orders of brown algae (Phaeophyceae) such as Laminariales, Fucales, Chordariales, Desmarestiales, Dictyotales. Their structures mainly consist of L-fucose backbone with glycosidic bonds. Apart from fucose and sulphate, they also contain mannose, glucoronic acid, xylose, galactose etc. (Berteau and Mulloy, 2003).

Some interesting pharmacological activities of fucoidans have been reported such as anti-inflammation (Yang *et al.*, 2006), anti-coagulant and anti-thrombotic activities (Cumashi *et al.*, 2007), anti-viral activity, anti-tumor (Li *et al.*, 2008) and anti-peptic ulcer (Shibata *et al.*, 2003) activities. Moreover, fucoidans are also applied as anti-aging and whitening agents in cosmetic applications (Fitton, Irhimeh and Falk, 2007).

Recently, the study on fucoidans for anti-tumor activities is widely attractive. For examples, fucoidans have been reported to suppress activator protein-1 (AP-1) activity and cell transformation induced by epidermal growth factor (EGF) in mouse epidermal (JB6 Cl41) cells (Lee *et al.*, 2008). Moreover, they could inhibit proliferation and enhance apoptosis in human lymphoma HS-Sultan cell line (Aisa *et al.*, 2005), inhibit the adhesion of human breast adenocarcinoma (MDA-MB-231) cells to fibronectin (Liu *et al.*, 2005), and significantly inhibit the growth of peripheral blood mononuclear cells in human T-cell leukemia virus (HTLV-1)-infected T-cell line (Haneji *et al.*, 2005).

Since, fucoidans have such advantages on cancer treatment and their structures contain sulphate groups which have ability to functionalize with the AuNPs; therefore, it is interesting to synthesize fucoidan-stabilized gold nanoparticles to improve the delivery of fucoidans to tumor sites and increase anti-tumor activities. Therefore, the present study was aimed to prepare and characterize of fucoidan-stabilized gold nanoparticles and to determine anti-tumor activities of the synthesized gold nanoparticles on the human lung adenocarcinoma (A549) cells.

2. Objectives of the study

2.1 To prepare and characterize of gold nanoparticles stabilized by algal fucoidans.

2.2 To determine the anti-tumor activities of fucoidan-stabilized gold nanoparticles on A549 lung cancer cell line.

CHAPTER II

LITERATURE REVIEW

1. Gold nanoparticles

1.1 Overview of gold nanoparticles

Nanotechnology was established in 1974 by a Japanese scientist Nario Taniguchi, who referred to tiny materials in the size range of 0.2-100 nm. "Nano-" derives from Greek meaning dwarf and 1 nanometer is equivalent to 10^{-9} meter (Dingler *et al.*, 1999). These nanoscaled materials exhibit unique properties which are different from macroscale properties. On an account of many advantages of nanoscaled materials, nanotechnology has rapidly emerged in various applications in the last few decades such as in electronics, communications, energy, household appliances, foods, medicines and cosmetics (Sanvicens *et al.*, 2008).

Metallic nanoparticles are inorganic nanoparticles which have long been attractive to scientists since historic times because they provide the brilliant colors. Since Egyptian and Roman time, metallic nanoparticles of gold (Au), silver (Ag) and copper (Cu) have been used by alchemists to stain glasses and for decorative artworks (Jain, El-Sayed and El-Sayed, 2007). Moreover, gold nanoparticles have long been used for therapeutic purposes in China and India. In India, gold colloid is known as Swarna Bhasma which is currently used for rejuvenation and anti-aging (Bhattacharya and Mukherjee, 2008).

The intense colors of metallic nanoparticles are caused by surface plasmon resonance of electron clouds around the metal atoms. Normally, electron clouds around metals are not strongly bound to the atomic cores (Figure 1). When the light of resonant wavelength is absorbed by the metal surfaces, the electron clouds will oscillate and scatter the energy. This phenomenon indicates that there are specific wavelengths in which the light cannot be reflected but absorbed and turned into the oscillation of electron clouds, known as surface plasmon resonance (SPR). In case of normal metal such as gold jewelry, these wavelengths occur in the infrared area (not in the visible area) of the spectrum resulting in shiny appearance. In contrast, nanoparticles have great high surface proportions therefore the specific wavelengths which light can be absorbed are shifted into visible area resulting in the different colors provided from normal metal. For example, gold nanoparticles absorb light in the blue-green portion at ~400-500 nm and reflect red light at ~700 nm, thus appearing red to the human eyes. As the sizes of Au particles increase, the absorbed lights are shifted to red light while the blue light is reflected, providing blue or purple color. This circumstance illustrates the interesting specific optical properties of metallic nanoparticles (Winter, 2007).

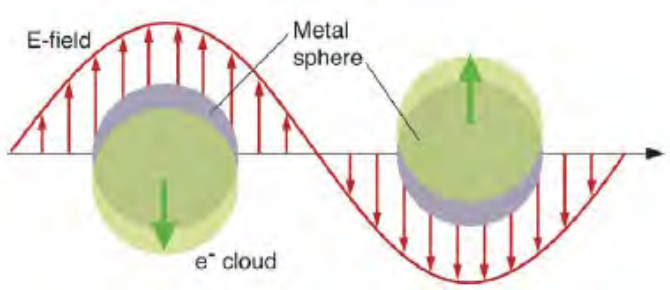

Figure 1 Schematic of interaction of electron cloud around metal nanosphere with light, electrons are not strongly bind to atomic core of metal, instead forming clouds (Jain *et al*., 2007).

Faraday firstly explained that the brilliant colors of these metallic colloids are caused by the nano-scale of metal particles. These interesting optical properties depend on their size and shape of the nanoparticles. Mie explained this phenomenon in 1908 by using Maxwell's electromagnetic equation to predict the optical properties of homogenous spherical nanoparticles. This equation is widely used to calculate the particle extinction spectra when the dielectric function of the material can be identified and the size of the tiny particles is much smaller than the light's wavelength (Link and El-sayed, 1999).

Gold (Au) and silver (Ag) nanoparticles are higher stable compared to copper (Cu) nanoparticles therefore they are the metal of choices. Interestingly, gold nanoparticles (AuNPs) are able to be synthesized in a wide range of size (4 – 80 nm) by simple methods (Jain *et al*., 2007). AuNPs can be synthesized using chemical, sonochemical, or photochemical techniques. The most common way to synthesize is *via* precipitation of Au ion in solution by reducing agents such as sodium citrate, ascorbic acid, sodium borohydride, or block-copolymer. Recently, previous study described sequential process of AuNP formation as a four-step nucleation and growth process. Briefly, the first step was a rapid formation of nuclei (a) and followed by the second step, rapid coalescence of the nuclei into bigger particles (b). The third step consisted of slow growth of particles along with reduction of gold atoms (c) and the last step was the rapid growth of nanoparticles to their final size (d) (Figure 2) (Polte *et al.*, 2010).

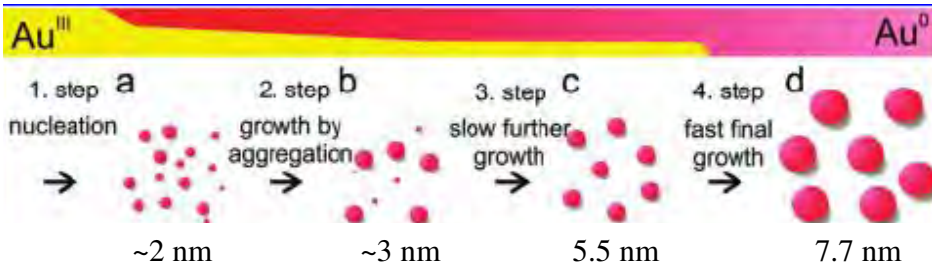

Figure 2 Schematic illustration for the reducing process of gold nanoparticle formation (Polte *et al.*, 2010)

After gold nanoparticles have been synthesized, they are usually furthered stabilizing by stabilizing agents to prevent aggregation of the nanoparticles (Polte *et al.*, 2010). Moreover, AuNPs are inert and biocompatible. Another advantage of AuNPs is due to their small size, they are able to pass easily into the cells and also penetrate through capillaries (Ghosh *et al.*, 2008).

1.2 Green synthesis of gold nanoparticles

As mentioned above, general AuNP synthesis required reducing agents such as sodium borohydride or other organic compounds which can be correlated with environmental toxicity and biological hazard. Therefore, increasing attention on green synthesis of metallic nanoparticles is of great interest. Thus, natural substances are an alternative way for metallic nanoparticle synthesis (Sun *et al.*, 2008). Recently, biopolymers including chitosan and dextran were successfully used for synthesis of metallic nanoparticles (Huang *et al.*, 2004; Nath *et al.*, 2008). In addition, some natural sources including marine alga (Singaravelu *et al.*, 2007) and fungus (Bhainsa *et al.*, 2006) are able to stabilize metallic nanoparticles.

1.3 Gold nanoparticles in medical areas

1.3.1 Bioimaging

Until now, finding new compounds with biocompatible properties is still challenging for imaging technique. Thus, AuNPs have gained much interest as a contrasting agent due to their non-toxic properties and intense SPR of the nanoparticles. AuNPs can act as colorimetric contrasting agents that have light scattering and absorption at the near infrared spectrum (NIR) ~700-1000 nm (Chen, Mwakwari and Oyelere, 2008). For examples, transferrin-conjugated AuNPs were used for targeting, imaging and therapeutic purposes of ductal carcinoma cells (HS 578T) and normal cells (3T3). The use of transferrin-conjugated AuNPs was six times higher in cellular uptake by the cancer cells compared to absence of this conjugation. Interestingly, the cellular uptake by normal cells was one fourth compared to the uptake by cancer cells (Li *et al.*, 2009). AuNPs conjugated with anti-epidermal growth factor receptor (EGFR) were successfully used for increasing in image intensity of cervical cancer cells (SiHa) (Rahman *et al.*, 2005).

1.3.2 Biosensing

Optical and electronic properties of AuNPs have been useful for detection of molecular events such as protein-protein interaction, protein aggregation and protein folding (Chen *et al.*, 2008). For examples, hepatitis B virus (HBV) DNA probes containing AuNPs used for direct detection of HBV with high sensitivity and simple operation (Xi *et al.*, 2007). AuNPs conjugated with anti-protein A (specific product of *Staphylococcus aureus*) were used for detection of *S. aureus* with rapid process and high sensitivity compared to conventional methods (Huang, 2007).

1.3.3 Photothermal therapy

Apart from special optical properties, AuNPs are able to generate a localized heat when they absorbed the light in range of 800-1200 nm (Ghosh *et al.*, 2008). This technique provides less invasive management for cancer therapy (Chen *et al.*, 2008). For example, AuNPs conjugated with anti-EGFR antibody showed selective destruction on oral squamous carcinoma cell lines (HSC 313 and HOC 3 clone 8) and a benign epithelial cell line (HaCaT) (El-Sayed, Huang and El-Sayed, 2006).

1.3.4 Drug delivery

AuNPs have been recently utilized in drug delivery system (DDS) due to their facile synthesis, controllable size, high stability and biocompatibility (Park *et al.*, 2009). Interestingly, surface of AuNPs are able to functionalize with organic molecules resulting in nano-drug preparation which can specifically deliver to target sites (Gibson, Khanal and Zubarev, 2007). Due to tiny size of AuNPs, they can be easily up-taken by cells *via* receptor-mediated endocytosis (RME) pathway. In case of some special surface chemistry, AuNPs can enter the cell by direct penetration without cell membrane disruption (Alkilany *et al.*, 2010). AuNPs conjugated with poorly water-soluble drugs such as ibuprofen and naproxen were developed in order to improve drug solubility (Hornig, Bunjes and Heinze, 2009). AuNPs conjugated with insulin could increase drug stability and enhance drug effects (Bhumkar *et al.*, 2007). AuNPs have been studied mainly on cancer therapy because nanocarrier of drug can accumulate preferentially in tumor sites more than in normal tissues, resulting in higher retention times and increasing drug effects; this phonomenon is known as the enhanced permeability and retention (EPR) effect. This EPR effect renders AuNPs to be a promising DDS for cancer therapy.

Many reports on AuNPs as DDS for anti-cancer approaches, polyethylene glycol (PEG)-coated AuNPs were biocompatible, less agglomerate and able to avoid from the immune system (Jain *et al*., 2007). Folate-modified thiolated PEG functionalized AuNPs have been used to conjugate with doxorubicin (Asadishad, Vossoughi and Alamzadeh, 2010), *cis*-platin (Patra, Bhattacharya and Mukherjee, 2009) and tamoxifen (Dreaden *et al.*, 2009). This form of AuNPs protected the normal cells from cytotoxic insults of cytotoxic drugs and enhanced the cytotoxic effects toward tumor cells. For AuNPs conjugated with β-lapachone, anti-cancer drug, the surface of AuNPs was functionalized with cyclodextrin, anti-EGFR and PEG. These AuNPs showed an improvement of intracellular uptake and apoptotic effect to cancer cells (Park *et al.*, 2009). AuNPs conjugated with kahalalide F showed high capacity to enter into the cells and enhanced cytotoxicity of drug (Hosta *et al.*, 2009).

Apart from mentioned utilizations of AuNPs as DDS, several anti-cancer activities have been reported to be arisen from the properties of AuNPs. For example, AuNPs inhibited the proliferation of vascular endothelial growth factor-165 (VEGF165)-induced human umbilical vein endothelial cells (HUVECs) and basic fibroblast growth factor (bFGF)-induced mouse embryonic fibroblast (NIH3T3) cells (Mukherjee *et al.*, 2005). VEGF165 and bFGF are heparin-binding growth factors which are important cytokine for angiogenesis. Whereas AuNPs did not inhibit an inducing effect by non-heparin-binding growth factors like VEGF121 and epidermal growth factor (EGF), suggesting that heparin-binding domain is crucial. AuNPs also suppressed the phosphorylation of vascular endothelial growth factor receptor (VEGFR)-2 which induced by VEGF165 and inhibited VEGF165-induced migration of HUVEC cells. For

in vivo, AuNPs inhibited VEGF165-induced permeability and angiogenesis in a nude mice ear model (Bhattacharya and Mukherjee, 2008). The apoptotic effect of AuNPs conjugated with anti-EGFR in B-chronic lymphocytic leukemia (BCLL) cell line has been reported. It was found that apoptosis were occurred in some cases after treatment with AuNPs alone (an AuNPs control group) supporting that AuNPs have anti-angiogenic properties (Mukherjee *et al.*, 2007).

As mentioned above, AuNPs are nanoparticles of choices for DDS of anti-cancer agents since many advantages of this DDS could be rendered due to EPR effect and easy penetration, providing an improvement of specific drug delivery to target sites and increasing cellular uptake capacity. These benefits result in enhancing drug efficacy and less toxicity to normal cells and decreasing in severe side effects from conventional cancer therapy. Moreover, anti-angiogenic properties of AuNPs could be useful for cancer treatment.

2. Cancer

Cancer is a group of serious diseases which involve uncontrollable cell proliferation. This disease can affect in many parts of the body such as skin, breast, gastro-intestinal system and liver. Cancer mortality rate in 2004 mounted to approximately 13% of all death worldwide (WHO, 2009). Lung cancer is a disease with very low five-year relative survival rate for all stages of disease (approximately 15%) due to a poor prognosis. The five-year survival rate was 49% for lung cancer detected at early stage however only 16% were diagnosed on early stage. (Jemal *et al.*, 2008). Currently, cancer treatments aim to get rid of all the abnormal cells, including

chemotherapy, radiation therapy and surgery which could cause the destruction of normal tissues and result in severe side effects for patients after each conventional therapy.

2.1 Metastasis

Metastasis is a multi-step of biological process involving the spreading of cancer cells from original site to other sites in the body. This phenomenon is concerned as cancer-related death in most cases of solid tumors. Briefly, cancer cells have to leave their primary site by migration or invasion through basement membrane and extracellular matrix and enter into lymphatic or circulatory systems. After the cancer cells travel along the circulations, they require adhesion to the wall of lymphatic or circulatory vessel and invade into the secondary site. Thus, metastasic cells are able to survive and grow in the distant organs (Figure 3) (Simpson, Anyiwe and Schimmer, 2008).

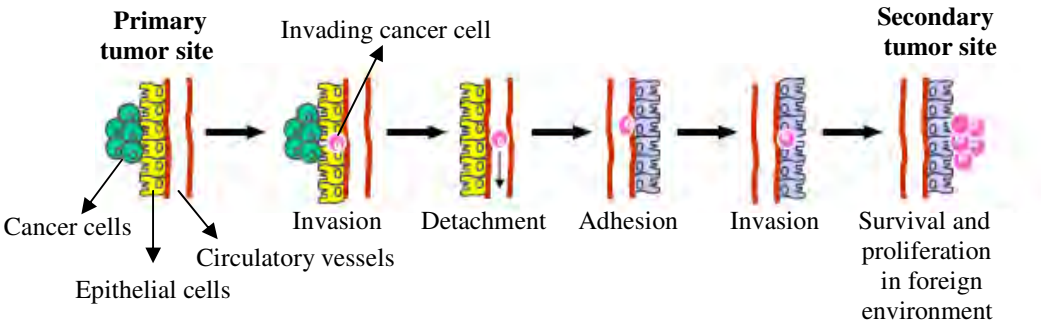

Figure 3 Metastasic steps of cancer cells from their primary site to secondary location (Simpson *et al.*, 2008)

2.1.1 Invasion process

Invasion process is a rate-limiting step of metastasis which involves the interaction between cancer cells and their environment including extracellular matrix (ECM) and basement membrane (BM). ECM is a non-living network which is located surroundingly by living tissues and this material provides structural support for living cells. BM is a particular form of ECM, situated on extracellular surface of epithelial cells and capillary endothelial cells. BM and ECM mainly consist of laminin, fibronectin, collagens, vitronectin and proteoglycans such as chondroitin sulphate, heparin sulphate and free hyaluronic acid (Brooks *et al.*, 2008).

In order to invade surrounding tissues, the cancer cells have to interact with the underlying BM as shown in Figure 4. Normally, epithelial cells are constrained by cell-cell contact or by BM (Figure 4A). Loss of cell-cell adhesion is occurred and the remodeling of ECM is taken place by the degradation of BM and ECM by proteolytic enzymes especially matrix metalloproteinases (MMPs) (Figure 4B). Degraded ECM is replaced by fibronectin or other ECM proteins which are recognized by the cancer cells (Figure 4C). Cancer cells switched their production of intermediate-filaments from keratin subtypes which are characteristic of fixed epithelial cells, to keratins and vimentin, promoting the fluid-like structure resulting in the induction of cell migration (Figure 4D). The combination of loss cell-cell contact, remodeling of ECM and altered expression of intermediate filaments and increasing cell motility bring about invasion of cancer cells through BM and ECM (Krishnamachary *et al.*, 2003; Semenza, 2003).

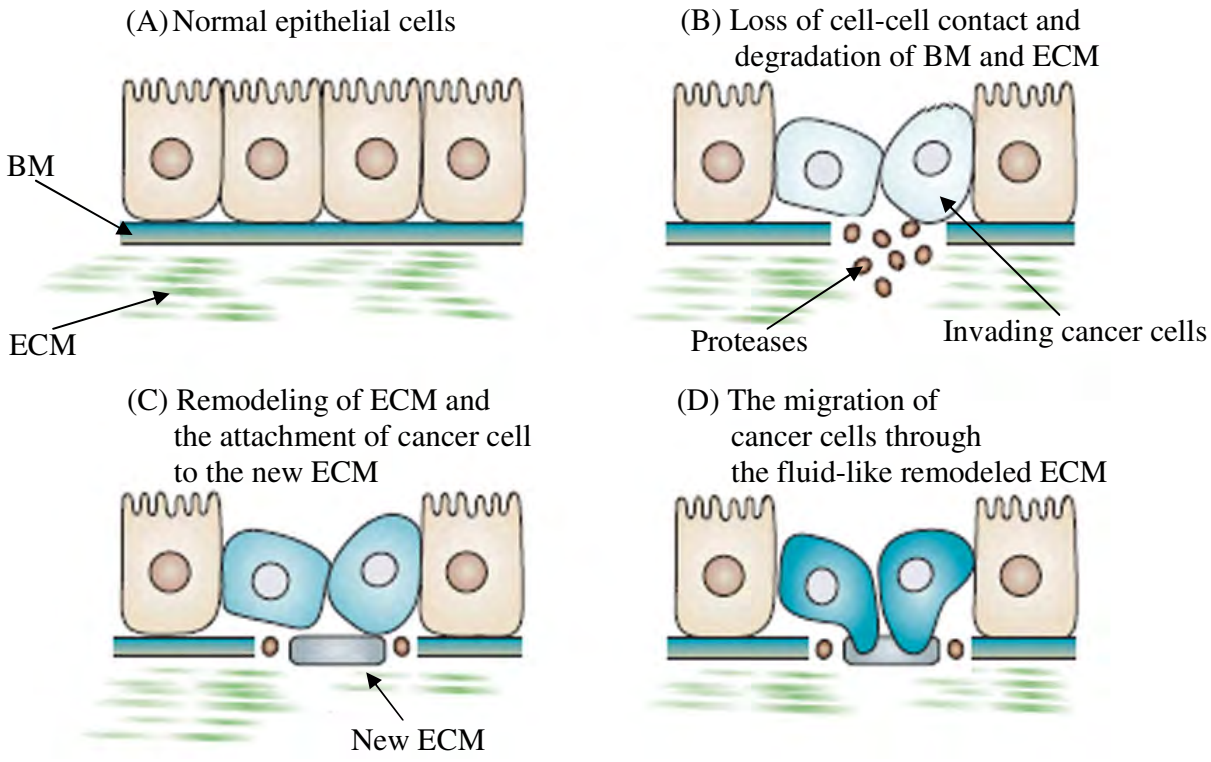

Figure 4 Schematic of tumor invasion (A) Epithelial cells are normally constrained by cell-cell contact and by BM. (B) The cancer cells secrete proteases to digest ECM and BM. (C) Degraded ECM is replaced by fibronectin or other ECM proteins which are recognized by the cancer cells. (D) Cancer cells switched their production of intermediate filaments from keratin subtypes which are characteristic of fixed epithelial cells, to keratins and vimentin, which promote the fluid-like structure (Semenza, 2003).

2.1.2 Anoikis resistance

Metastasis of cancer cells requires the epithelial cells to separate from their primary site and invade into lymphatic or circulatory systems. Normally, the attachment of epithelial cells to extracellular matrix (ECM) provides survival signaling. When the

cells lose their attachment (detachment), they will undergo apoptosis and this form of programmed cell death is known as anoikis (Wang, 2004).

However, some cancer cells are able to survive and grow in the lack of attachment to the ECM and their neighboring cells. Thus, resistance of anoikis is concerned to be the most important process for allowing the cancer cells metastasize to secondary organs (Wang, 2004). Previous studies showed that four different ovarian cancer cell lines in monolayer and multicellular tumor spheroid conditions were treated with paclitaxel. The spheroid culture of cancer cells did not response to paclitaxel whereas they did in monolayer culture (Frankel, Buckman and Kerbel, 1997). Moreover, human hepatoma (BEL7402 and SMMC7721) cell lines were treated with 5-flurouracil (5-FU), TRAIL (apoptosis-induced ligands) and UV-radiation in monolayer and suspended cells. The results showed that suspended hepatoma cells were more resistant to 5-FU, TRAIL and UV-radiation than monolayer culture (Zhang *et al.*, 2008).

3. Fucoidans

In 1913, Kylin first isolated sulphated polysaccharides obtained from marine brown algae and named the compound as “fucoidin”. According to IUPAC rules, they are called fucoidan and this natural substance also known as sulphate fucan, fucosan or fucan. Furthermore, in 1984, Vasseur reported that these polysaccharides are also present in some marine invertebrates (Li *et al.*, 2008).

3.1 Sources of fucoidans

The natural polysaccharides, fucoidans, are found in cell wall of marine brown algae and in marine invertebrates such as egg jelly coat of sea urchins and body wall of sea cucumbers. Fucoidans widely present in several orders of marine brown algae (Phaeophyceae) such as Laminariales, Fucales, Chordariales, Desmarestiales, Dictyotales. Fucoidans are easily extracted *via* hot water or acid solution, these methods allow extraction of the polysaccharides by more than 40% of the dry weight of the isolated cell wall (Berteau and Mulloy, 2003).

3.2 Fucoidan structures

Fucoidan structures are mainly consisted of sulphated L-fucose backbone with glycosidic bonds. Apart from fucose and sulphate, other constituents include mannose, glucoronic acid, xylose, galactose etc. In 1954, O'Neil reported that the basic structure of fucoidan obtained from *Fucus vesiculosus* was α-(1→2)-fucose and sulphate groups were mostly present at a position C-4 of the fucose units (O'Neil, 1954). However, in 1993, Patankar and coworkers suggested that the core structure of fucoidan obtained from the same brown alga specie as in a previous study was α-(1→3) linked fucose with sulphate groups at a position of some C-4 fucose units; additionally fucose also formed branch chains to this polymer. The different structures of fucoidan may be due to the difference in extraction method and analysis techniques (Patankar *et al.,* 1993). Moreover, Sugar composition and structures of fucoidans vary depending on species of marine brown algae and climatic agriculture. Previous studies showed that structures of algal fucoidans are very complex and consists of multiple branches whereas sulphated polysaccharides obtained from marine invertebrates are regular and straight (Berteau and Mulloy, 2003).

The structure of algal fucoidan obtained from *Cladosiphon okamuranus* mainly consists of α-(1→3) linked fucose with sulphate groups and glucoronic acid as additional groups (Figure 5) (Sakai *et al.*, 2003). However, the structures of algal fucoidans obtained from *Kjellmaniella crassifolia* may comprise of three different structures (Figure 6) (Takara Bio Inc, 2009). As shown in Figure 6, sugar composition of algal fucoidan prepared from *K. crassifolia* contains fucose, glucoronic acid and galactose. Besides sugar composition differences, the position of additional sulphate groups also varies. Algal fucoidan obtained from *C. okamuranus* has sulphate position at C-4 whereas sulphate positions in algal fucoidans obtained from *K. crassifolia* vary in different structures.

As mentioned above, structures of fucoidan obtained from marine brown algae are heterogenous and contain many branch chains. It is important to note that structures of algal fucoidans vary from species to species of marine brown algae and these different structures would affect sorting and potency of their biological activities (Li *et al.*, 2008).

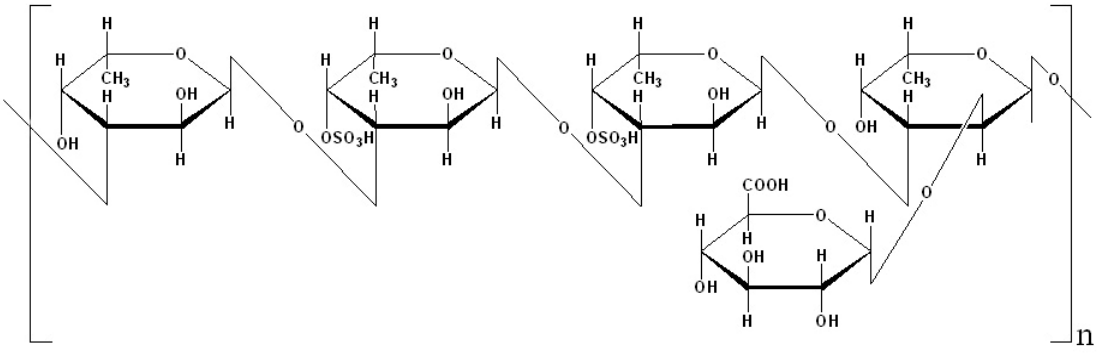

Figure 5 Structure of algal fucoidan obtained from *C. okamuranus* is a repeating unit of (-3L-Fuc-α-(1→3)-L-Fuc(4-*O*-sulphate)-α-(1→3)-L-Fuc(4-*O*-sulphate)-α-(1→3)(D-GlcA-α-(1→2)-L-Fuc-α-1-) (Sakai *et al.*, 2003).

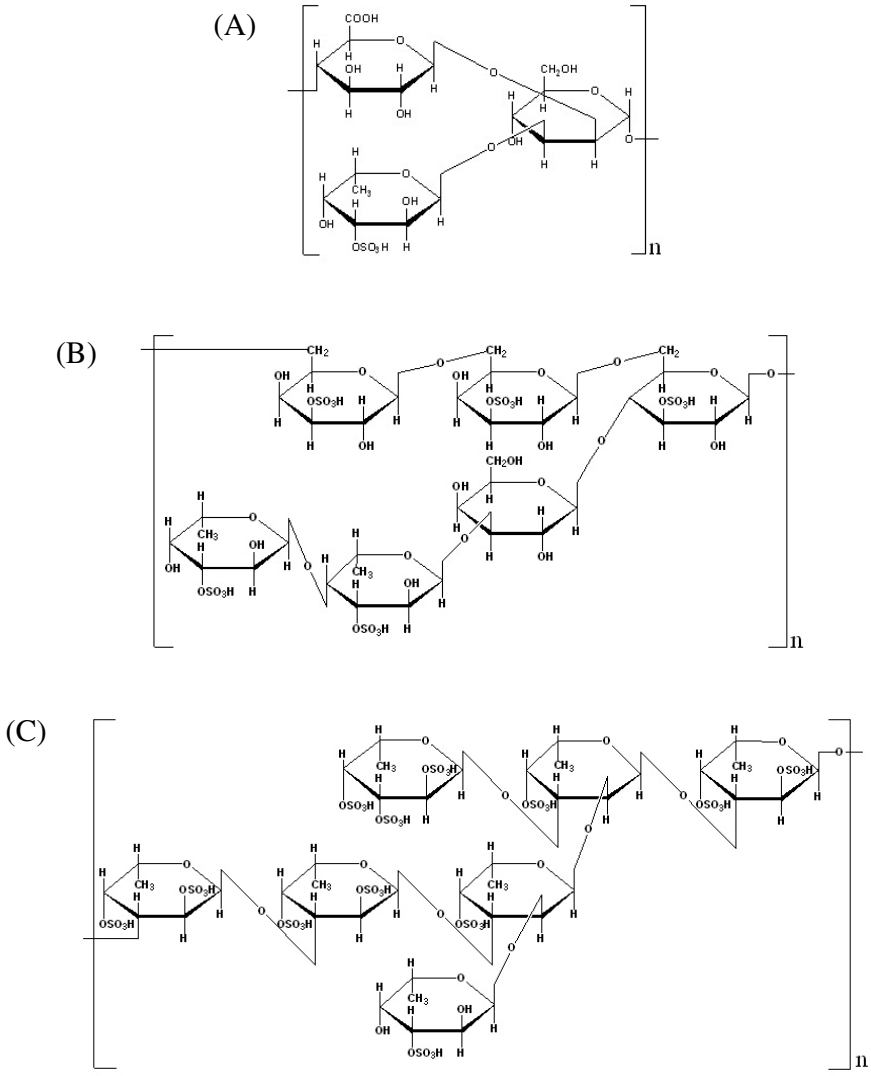

Figure 6 Three different structures of algal fucoidan obtained from *K. crassifolia*; structure (A) is a repeating unit of (-4L-GlcA-α-(1→2)(L-Fuc(3-*O*-sulphate)-α-(1→3)-D-Gal-α-1-), structure (B) is a repeating unit of (-6-L-Fuc(3-*O*-sulphate)-α-(1→6)-L-Fuc(3-*O*-sulphate)-α-(1→6)((L-Fuc(3-*O*-sulphate)-α-(1→4)-L-Fuc(3-*O*-sulphate)-α-(1→3)-L-Fuc-α-(1→4))-L-Fuc(3-*O*-sulphate)-α-1), and structure (C) is a repeating unit of (-3L-Fuc(2,4-*O*-sulphate)-α-(1→3)-L-Fuc(2,4-*O*-sulphate)-α-(1→3)((L-Fuc(3-*O*-sulphate)-α-(1→2))-L-Fuc(4-*O*-sulphate)-α-(1→2)((L-Fuc(2,3,4-*O*-sulphate)-α-(1→3))-L-Fuc(4-*O*-sulphate)-α-(1→3)-L-Fuc(2,4-*O*-sulphate)-α-1-) (Takara Bio Inc, 2009).

3.3 Biological activities of fucoidans

Some interesting pharmacological activities of algal fucoidans have been reported as follows;

3.3.1 Anti-coagulant and anti-thrombotic activities

Structures of algal fucoidans are similar to heparin, renowned anti-coagulant drug obtained from natural sources. Therefore, algal fucoidans are considerate to be heparin-like compounds which present anti-coagulant and anti-thrombotic activities with less in side effect compared to heparin. Many studies showed that anti-coagulant property of fucoidans related to content and position of sulphate groups, sugar composition and molecular weight of the polysaccharides (Li *et al.*, 2008). In 2007, Cumashi and coworkers compared the anti-coagulant and anti-thrombotic properties of fucoidans obtained from nine different species of marine brown algae. They indicated that algal polysaccharides obtained from *Laminaria saccharina, L. digitata, Fucus serratus,* and *F. distichus* showed potent anti-coagulant property (Cumashi *et al.*, 2007). While, fucoidans obtained from *F. spiralis*, *F. evanescens, F. vesiculosus,* and *Ascophyllum nodosum* exhibited moderate activity and fucoidan obtained from *C. okamuranus* presented very low activity. The different potency was possibly due to the lower content of sulphate in the latter fucoidan and the structural feature that contains glucoronyl substituents was distinct from other fucoidans. Another study compared hemorrhagic effect of heparin and fucoidans obtained from *F. vesiculosus*. The results suggested that fucoidans had lower hemorrhagic effect compared to heparin in *in vivo* assay (De Azevedo *et al.*, 2009).

3.3.2 Anti-peptic ulcer

Algal fucoidans prepared from *C. okamuranus* showed protective effects against *Helicobacter pylori* on attachment to gastric mucosa in both *in vitro* and *in vivo* assays. These polysaccharides competitively bind to bacterial surface against gastric mucin (Shibata *et al.*, 2003).

3.3.3 Anti-inflammation

Fucoidans obtained from *C. okamuranus* and *K. crassifolia* showed reduction of interleukin (IL)-6 production in lipopolysaccharide (LPS)-stimulated murine colonic epithelial cells (CMT-93) with the down regulation of NF-κB nuclear-translocalization in LPS-stimulated CMT-93 cells. Fucoidan from *C. okamuranus* also decreased IL-6 and interferon (IFN)-γ and increased IL-10 and transforming growth factor (TGF)-β in rat model (Matsumoto *et al.*, 2004). Moreover, Cumashi and coworkers showed that fucoidans from marine brown algae (*Laminaria saccharina, L. digitata, Fucus evanescens, F. serratus, F. distichus, F. spiralis*, *Ascophyllum nodosum* and *C. okamuranus*) at 4 mg/kg oral dose presented inhibition of neutrophil extravasation into the peritoneal cavity in an acute peritonitis rat model. Moreover, fucoidans from *F. distichus* and *F. spiralis* were less active compounds compared to other fucoidans. However, there was no relationship between anti-inflammatory effect and the structural feature of fucoidan (Cumashi *et al.*, 2007).

3.3.4 Anti-viral activities

Algal polysaccharide from *Undaria pinnatifida* showed inhibitory effect against herpes simplex virus (HSV) type 1 replication in *in vitro* and stimulated immune system function after oral administration in mice (Hayashi *et al.*, 2008). Likewise, fucoidans from *Sargassum tenerrimum* and *Panida tetrestromatica* were observed to have anti-viral activities on HSV-1 and HSV-2. The results indicated that higher content of sulphate in fucoidans exhibited potent inhibitory activities against HSV-1 and HSV-2 (Karmakar *et al.*, 2010; Sinha *et al.*, 2010).

3.3.5 Anti-tumor activities

Many fucoidans from different species of marine brown algae have been investigated on anti-tumor activities in various cell lines. Fucoidan obtained from *F. vesiculosus* induced apoptosis of human HS-Sultan cells *via* activation of caspase-3 and down-regulation of extracellular signal-regulated kinases (ERK) pathways (Aisa *et al.*, 2005). Moreover, this fucoidan also has growth inhibitory effects on human colon carcinoma cells (HCT-15) by inducing apoptosis *via* activation of ERK, p38 and inhibition of PI3K/Akt in a time-dependent manner (Hyun *et al.*, 2009). Fucoidan prepared from *U. pinnatifida* showed cytotoxic effect on prostate cancer (PC-3) cells, cervical cancer cells (HeLa), human alveolar basal epithelial cell carcinoma (A549) cells and hepatocellular carcinoma (HepG2) cells (Synytsya *et al.*, 2010). Fucoidan extracted from *C. okamuranus* showed growth inhibitory effects on various cell lines including hepatocellular carcinoma, cholangiocarcinoma and gall bladder carcinoma whereas no growth inhibitory effects was found on neuroblastoma and ovarian carcinoma cell lines (Fukahori *et al.*, 2008). Additionally, fucoidan obtained from *C. okamuranus* also

inhibited the growth of peripheral blood mononuclear cells in human T-cell leukemia virus (HTLV-1)-infected T-cell line (Haneji *et al.*, 2005). Furthermore, enzyme-digestion of fucoidan extracted from *C. novae-caledoniae kylin* also inhibited the invasion of human fibrosarcoma (HT1080) cell line possibly *via* suppression of matrix metalloproteinase (MMPs) -2 and -9 and angiogenesis *via* inhibition of expression of vascular endothelial growth factor (VEGF) (Ye *et al.*, 2005). Fucoidan prepared from *Ascophyllum nodosum* had cytotoxic effect on African green monkey kidney (Vero) and rat sarcoma (XC) cell lines (Jiang *et al.*, 2010) as well as inhibited the adhesion of human breast adenocarcinoma (MDA-MB-231) cells to fibronectin (Liu *et al.*, 2005). In contrast, anti-adhesive effect was not found in MDA-MB-231 attached to immobilized platelet after treatment with fucoidans obtained from *C. okamuranus* and *F. spiralis* (Cumashi *et al.*, 2007). Algal fucoidans from *Spatoglossum schröederi* also showed an inhibitory effect on adhesion of wild-type Chinese hamster ovary cells (CHO-K1) and xylosyltransferase-deficient mutant (CHO-741) cells to fibronectin while the desulphated form of this fucoidan did not show any inhibitory effect on adhesion of those cell lines (Rocha *et al.*, 2005). On the contrary, this effect was not found on the attachment of these ovarian cancer cells to laminin whereas adhesion to vibronectin was inhibited on CHO-K1 cells and adhesion to type I collagen was suppressed in CHO-745 cells (Rocha *et al.*, 2001). Fucoidan prepared from *Larminaria guryanovae* has been reported to suppress activator protein-1 (AP-1) activity and cell transformation induced by epidermal growth factor (EGF) in mouse epidermal (JB6 Cl41) cells (Lee *et al.*, 2008). As mentioned above, it is important to note that anti-tumor activities of algal fucoidans

depend on many factors including species of marine brown algae, sulphate content, sugar composition of algal fucoidans and cancer cell types.

3.4 Fucoidan safety

Algal fucoidans have a wide-spectrum of interesting bioactivities, so fucoidan demand has increased for functional foods and drug developments from natural sources. The toxicity of algal fucoidans has been examined to ensure the safety after use of these compounds. Fucoidan obtained from *U. pinnatifida* has been tested on the toxicity of a 4-week oral trial in Sprague-Dawley (SD) rats. After treatment of SD rats with fucoidan (1,350 mg/kg/day), no significant differences in body weight, ophthalmoscopy, urinalysis, hematology and histopathology were observed and also unchanged in pro-thrombin time or activated partial thromboplastin time (Kim *et al.*, 2009). The acute toxicity of fucoidan extracted from *C. okamuranus* has been investigated in Wistar rats after oral administration. At 600 mg/kg of body weight, fucoidan did not induce toxicological changes but at a dose of 1,200 mg/kg of body weight, fucoidan has a prolonged effect on clotting time (Gideon and Rengasamy, 2008).

As mentioned previously, fucoidans are natural polymer abundant in sulphate as additional groups and have many bioactivities. Fucoidans have a potential to act as reducing and stabilizing agents in AuNP synthesis. Therefore, this study is aim to prepare AuNPs conjugated with fucoidans and to study the anti-tumor activities of fucoidan-stabilized AuNPs on lung cancer cell line (A549). These nano-scaled fucoidans might be potentiated the anti-tumor effects and useful for cancer therapy.

CHAPTER III

MATERIALS AND METHODS

1. Materials

1.1 Equipment

1. 24-well plate (Costar, USA)
2. 96-well plate (Nunc, Denmark)
3. Balance (AG204, Mettler Toledo, Switzerland)
4. Cell culture plate (Nunc, Denmark)
5. CO_2 incubator (Thermo Scientific, USA)
6. De-ionized water (DI water) system (ELGAStat Option 3B) (ELGA, England)
7. Electrophoresis apparatus (3000Xi, Biorad, USA)
8. Membrane filter (0.2 µm pore size) (Pall Corporation, USA)
9. Micropipettes SL-20 (2-20 µL), SL-200 (20-200 µL) and SL-1000 (100-1,000 µL) (Rainin Instrument, USA)
10. Micropipettes tips (Gibson, France)
11. Microplate reader ($SPECTRA_{max}$ $Plus^{384}$, Molecular Devices, USA)
12. Multichannel pipettes (Gibson, France)
13. Refrigerated centrifuge (Himac CR20B3, Hitachi, Japan)
14. Spectrophotometer (UV-160A, Shimadzu, USA)
15. Transmission Electron Microscopy (TEM) with energy dispersive X-ray spectroscopy (EDS) attachment and specimen heating holder (JEM-2100, Jeol, Japan)

16. Transwell® attached with polycarbonate membrane filter (8.0 µm pore size) (Corning, USA)
17. Ultracentrifuge (Optima L-80, Beckman Coulter, USA)
18. Ultra-purifier water system (Maxima UF, England)
19. Vortex mixer (Clay Adams, USA)
20. Zetasizer NanoZS (ZEN3600, Malvern, UK)

1.2 Chemicals

1. Acetic acid (Sigma-Aldrich, USA)
2. Acrylamide (Biorad, USA)
3. Ammonium persulfate (Sigma-Aldrich, USA)
4. Antibiotic-antimycotic (Gibco, USA)
5. Calcium chloride (Sigma-Aldrich, USA)
6. Coomassie brillilant blue (Serva, Germany)
7. Crystal violet (Fluka, Switzerland)
8. Dimethylsulfoxide (DMSO) (Merck, Germany)
9. Eagle's minimal essential medium (DMEM) (Invitrogen, USA)
10. Ethanol (Sigma-Aldrich, USA)
11. Fetal bovine serum (Gibco, USA)
12. Fibronectin (Sigma-Aldrich, USA)
13. Gelatin (Sigma-Aldrich, USA)
14. Hydrochloric acid (Sigma-Aldrich, USA)
15. Hydrogen tetrachloroaurate trihydrate ($HAuCl_4.3H_2O$) (Sigma-Aldrich, USA)

16. Matrigel® (Becton Dickinson, USA)
17. Methanol (Sigma-Aldrich, USA)
18. Methylene blue (Carlo Erba Reagents, Italy)
19. 3-(4,5-dimethylthiazol-2-yl)-2,5-diphenyl tetrazolium bromide (MTT) (Sigma-Aldrich, USA)
20. Nitric acid (HNO_3) (Carlo Erba Reagents, Italy)
21. Okinawa Mozuku fucoidan (Meiji Food Materia, Japan)
22. Poly-HEMA (poly(2-hydroxyethyl methacrylate) (Sigma-Aldrich, USA)
23. Roswell Park Memorial Institute medium (RPMI) (Invitrogen, USA)
24. Sodium azide (Fluka, Switzerland)
25. Sodium dodecyl sulfate (SDS) (Sigma-Aldrich, USA)
26. Takara Kombu fucoidan (Takara Bio, Japan)
27. Trisodium citrate dihydrate ($Na_3C_6H_5O_7.2H_2O$) (Sigma-Aldrich, USA)
28. Triton X-100 (USB, USA)
29. Trypan blue (Sigma-Aldrich, USA)
30. Ultrapure water (18.2 MΩ) (Elga, UK)

1.3 Cell lines

1. Human embryonic lung fibroblast cells (MRC-5) (The American Type Culture Collection (ATCC), USA)
2. Human lung adenocarcinoma cells (A549) (The American Type Culture Collection (ATCC), USA)

2. Methods

2.1 Preparation of AuNPs

Before preparing AuNPs, all glassware were washed to remove gold contamination using aqua regia ($HCl:HNO_3$ = 3:1) and followed by rinsing with ultrapure water and oven dried.

2.1.1 Preparation of fucoidan-stabilized AuNPs

In this study, fucoidan-stabilized AuNPs were prepared using commercial sulphated polysaccharides extracted from marine brown algae, Takara Kombu fucoidan (TK fucoidan) and Okinawa Mozuku fucoidan (OM fucoidan), which were obtained from *Kjellmaniella crassifolia* and *Cladosiphon okamuranus*, respectively.

The preparation of AuNPs was modified from Nath *et al*. (2008). To obtain the optimum ratio of gold (Au atom) to fucoidan, different amounts of fucoidan (0.1 – 1.2 mg/ml) were dissolved in deionized water. Then, 30% w/w hydrogen tetrachloroaurate (III) trihydrate ($HAuCl_4.3H_2O$) solution was added to obtain 0.1 mM (19.7 ppm) of Au atom. The mixture was then heated at 80^{o}C on a water bath with magnetic stirrer for 45 mins (Figure 7). Alternatively, the mixture was stirred at room temperature (25^{o}C) until the sample changed to pink color. The obtained solid nanoparticles were kept in a refrigerator.

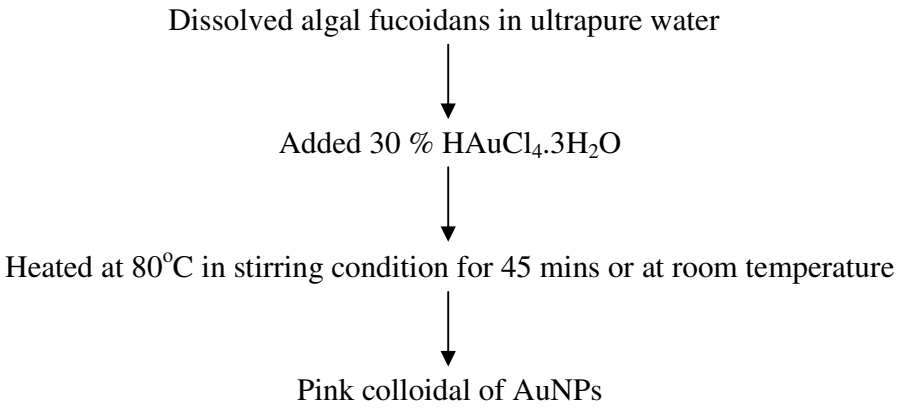

Figure 7 Preparation of fucoidan-stabilized AuNPs

2.1.2 Preparation of citrate-stabilized AuNPs

Citrate-stabilized AuNPs (Cit-AuNPs) were synthesized and used to compare with the fucoidan-stabilized AuNPs. The synthesis procedure was modified from the method of Kimling *et al.* (2006). Briefly, 30% w/w $HAuCl_4.3H_2O$ was added into ultrapure water. The mixture containing 2 mM Au was heated up to 80°C and then, 0.202 M trisodium citrate dihydrate ($Na_3C_6H_5O_7.2H_2O$) was added and the solution was continued heating until the deep red solution was obtained.

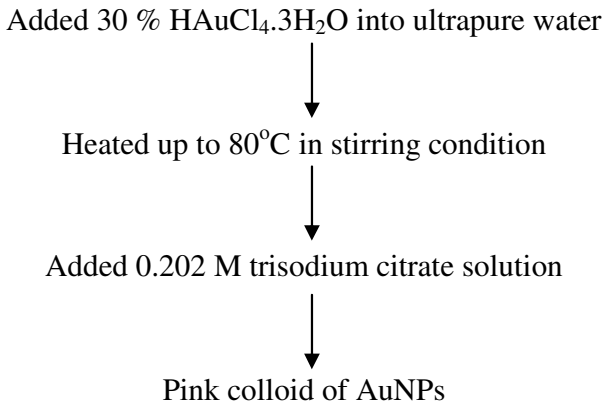

Figure 8 Preparation of citrate-stabilized AuNPs

2.2 Characterization of fucoidan-stabilized AuNPs

UV-Visible spectroscopy was used for measuring the surface plasmon resonance of the AuNPs. The observed wavelength is in the range of 400-800 nm. Transmission Electron Microscopy (TEM) (JEM-2100 with 200 kV) was used to obtain the image of the AuNPs and Semafore 4.01 demo software (Joel Co., USA) was used to determine average particle size and size distribution of the nanoparticles. Elemental analysis was conducted using X-ray energy dispersive spectroscopy (EDS) in conjunction with TEM. The zeta potential of the AuNPs was measured using Zetasizer Nano ZS. In order to study the stability of AuNPs after one-month storage, AuNPs were observed for their separation and characterized by previously mentioned methods including UV-Visible spectroscopy, TEM and zeta potential measurement.

2.3 Estimation of fucoidan amount in fucoidan-stabilized AuNPs

To estimate amount of fucoidans in the AuNPs, the quantitative method was modified from the experiment of Jiao and Liu (1999). The algal polysaccharides are able to form complex with methylene blue which would be detected by the decreased absorbance after the reaction. Briefly, fucoidans were diluted to obtain the final concentration in a range of 0 – 3 µg/ml. Then, 150 µl of 0.0275% w/w methylene blue solution was added and the UV absorbance was measured at different concentrations of fucoidan for obtaining a calibration curve. The supernatant of AuNP colloid obtained after ultracentrifugation at 25,000 rpm for 20 mins was measured and the absorbance was calculated to obtain the concentration of fucoidan. The amount of fucoidan in the AuNPs

was evaluated by subtraction of the amount of fucoidan in the supernatant from the total amount of fucoidan in AuNP colloid.

2.4 Study on anti-tumor activities of fucoidan-stabilized AuNPs

2.4.1 Preparation of samples

Fucoidan-stabilized AuNPs were freshly prepared and ultra-centrifuged at 25,000 rpm for 20 mins to get rid of the excess stabilizer and resuspended in deionized water before testing. The fucoidan-stabilized AuNPs used for the study contained fucoidan at the concentration of 30, 100 and 300 µg/ml. Moreover, fucoidan solution (30, 100 and 300 µg/ml) and Cit-AuNPs (no fucoidan added) at the same concentrations of Au in the fucoidan-stabilized AuNPs were also tested for cytotoxicity and anti-tumor activities on A549 cell line.

2.4.2 Cell cultures

Human lung adenocarcinoma cells (A549) and human embryonic lung fibroblast cells (MRC-5) were grown in RPMI-1640 and DMEM media, respectively. The media were supplemented with 10% of fetal bovine serum (FBS), 100 U/ml penicillin, 100 µg/ml streptomycin, and 12.5 µg/ml amphotericin B, and maintained at 37^{o}C in a humidified 5% CO_2 atmosphere. The conditioned medium obtained from MRC-5 cells was used in invasion and cell migration assay. To prepare MRC-5 conditioned medium, the culture medium was collected from confluent MRC-5 cells culture and sterilized by filtration through 0.2 µm membrane filters, and kept at -20^{o}C.

2.4.3 Cytotoxic assay

MTT (3-(4,5-dimethylthiazol-2-yl)-2,5-diphenyl tetrazolium bromide) assay was a method used to determine cell viability. The MTT method was modified from the method of Alley *et al*. (1988). MTT, yellow tetrazolium salt is able to dissolve in culture media and it can be changed to formazan product (a water-insoluble compound) by mitochondrial reductase in viable cells and detected by measuring absorbance using a microplate reader. Briefly, the suspension of A549 cells was seeded into each 96-well plate (3×10^4 and 5×10^3 cells/well for one day and three days of treatment, respectively) and incubated overnight to allow the cells to attach the 96-well plate. After that, cells treated with fucoidans, citrate-stabilized AuNPs or fucoidan-stabilized AuNPs were performed for one-day or three-day incubation. The cells without any sample added were used as a control. Then, the media in each well were replaced by 100 µl of culture media containing 0.5 mg/ml MTT in each well and incubated for two hours at 37°C in a humidified 5% CO_2 atmosphere. Next, the media in each well were aspirated, the cells were lysed and the formazan product was dissolved by adding 100 µl dimethyl sulfoxide (DMSO). The absorbance (A) was measured at 550 nm using a microplate reader with the reference absorbance at 650 nm. The experiment was run in triplicate and the results were expressed as percentage of cell viability compared with a control (untreated group). $A_{(Blank)}$ was obtained from a group containing only media (no cell and sample added).

$$\% \text{ Cell viability} = \frac{A_{(sample)} - A_{(blank)}}{A_{(control)} - A_{(blank)}} \times 100 \quad \text{—— (1)}$$

2.4.4 Anoikis resistance assay

Since cancer cells are able to survive in anchorage-independent condition and spread to other organs, anoikis resistance is considerate to be a major requirement for metastasis. Therefore, cytotoxic effect of fucoidan-stabilized AuNPs in detached A549 cells was also investigated using poly-HEMA (poly(2-hydroxyethyl methacrylate) coated 96-well plate to prevent the cells from plate attachment. For anoikis resistance assay, the method of Fukazawa *et al.* (1995) was followed with some modifications. The suspension of A549 cells (3 x 10^4 cells/100µl/well) was incubated with fucoidans, citrate-stabilized AuNPs or fucoidan-stabilized AuNPs for one or three days in the poly-HEMA coated plates. After treatment, 25 µl of MTT solution (5.5 mg/ml) was added into each well to obtain 0.5 mg/ml MTT in each well and the plate were further incubated for 2 hours at 37^{o}C in a humidified 5% CO_2 atmosphere. Then, spheroid A549 cells were lysed and the formazan product was dissolved by addition of 100 µl of 20% sodium dodecyl sulfate (SDS) in 10 mM HCl and left overnight. The absorbance at 550 nm was measured using a microplate reader with the reference absorbance at 650 nm. The results were expressed as percentage of cell viability compared to a control (untreated cells).

2.4.5 Invasion and cell migration assay

To evaluate an inhibitory effect of the AuNPs on invasion and cell migration, Transwell® attached with polycarbonate membrane filter (8.0 µm pore size) was used to determine invasion and cell migration capability of cancer cells (Lirdprapamongkol *et al.*, 2005). In the studies, the membrane filters were pre-coated with fibronectin (1 µg/filter) at the lower surface of membrane filters to prevent the cells from falling down to the lower chamber. In case of invasion assay, membrane filters were pre-coated with the

cellular ECM, Matrigel® (30 µg/filter), before use. MRC-5 conditioned medium was used as a chemoattractant which was able to induce the cancer cells in the upper chamber to invade or migrate through the membrane filter and attached at the lower surface of membrane (Figure 9). Then, the cells at the lower part of a membrane were stained and determined for a number of invading or migrating cells. The 200 µl of A549 cell suspension (1 x 10^5 cells) was mixed with fucoidans, citrate-stabilized AuNPs and fucoidan-stabilized AuNPs and then added on the upper chamber of Transwell®. Then, MRC-5 conditioned medium containing the same concentrations of the test samples was added into the lower part of Transwell® and incubated at 37°C in a humidified 5% CO_2 atmosphere for 6 hours. After incubation period, the remaining A549 cells in the upper chamber were eliminated by wiping with cotton buds, whereas the cells attached on the lower surface of membrane filter were fixed with 25% methanol solution and stained with 0.5% crystal violet in 25% methanol solution. Then, the filters were cut off and placed into 96-well plate. The retaining dye on the lower part of membrane was extracted by 0.1 N HCl in methanol and the absorbance was determined at 550 nm using a microplate reader. Cell migration assay was performed in the same way except using membrane filter without Matrigel® coated. The results were expressed as percentage of invasion or cell migration compared to a control (untreated cells). $(A)_{Blank}$ was obtained from a group containing only media (no cell and sample added).

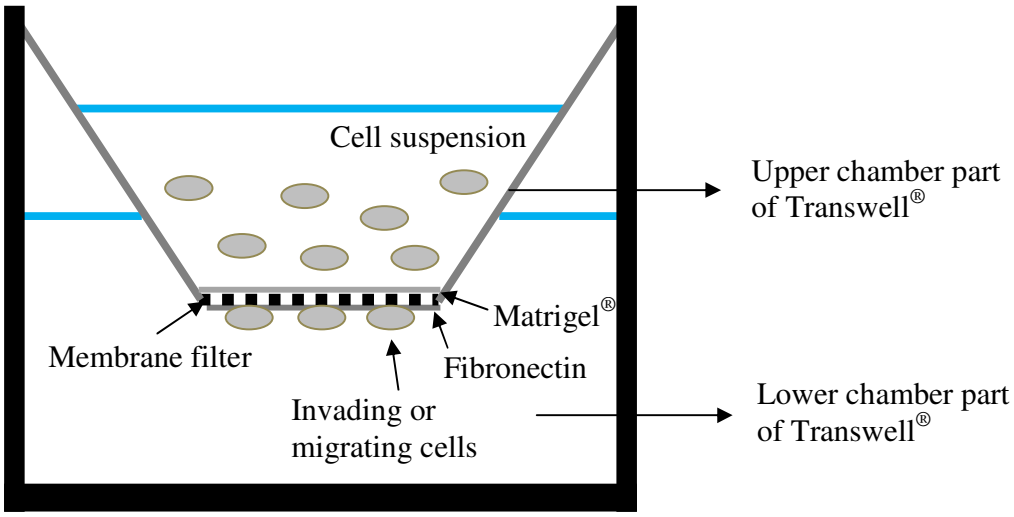

Figure 9 The schematic diagram of invasion assay

$$\% \text{ invasion or cell migration} = \frac{A_{(sample)} - A_{(blank)}}{A_{(control)} - A_{(blank)}} \times 100 \quad \text{—— (2)}$$

2.4.6 Cell adhesion assay

This study was to evaluate whether the AuNPs have any inhibitory effect on cell-ECM adhesion; Matrigel®-coated and fibronectin-coated 96-well plates were used with some modifications (Kikkawa, Sanzen and Sekiguchi, 1998). Briefly, 100 µl cell suspension of A549 cells ($4x10^4$ cells) containing fucoidans, citrate-stabilized AuNPs and fucoidan-stabilized AuNPs was seeded into each well and incubated at 37°C in a humidified 5% CO_2 atmosphere for an hour. After that, A549 cells were washed with phosphate buffered saline (PBS) and fixed with 95% ethanol, followed by staining with crystal violet solution. Then, the stained A549 cells were extracted by freshly

preparation of 0.1 N HCl in methanol and absorbance was determined at 550 nm using a microplate reader. The results were expressed as percentage of adhesion compared to a control (untreated cells). $(A)_{Blank}$ was obtained from a group containing only media (no cell and sample added).

$$\% \text{ adhesion} = \frac{A_{(sample)} - A_{(blank)}}{A_{(control)} - A_{(blank)}} \times 100 \quad \text{(3)}$$

2.4.7 Matrix metalloproteinase-2 and -9 production assay

Matrix metalloproteinase-2 and -9 (MMP-2 and MMP-9) are considered to be major enzymes which used to digest the extracellular matrix (ECM) during invasion process. Therefore, the inhibitory effect on MMPs production of fucoidan-stabilized AuNPs was investigated and the gelatin zymography was used in this study (Lee *et al.*, 2003). The A549 cells were cultured overnight in 24-well plate ($1x10^5$ cells/well), followed by washing the wells twice with serum-free media. Then, A549 cells were incubated in serum-free media containing fucoidans, citrate-stabilized AuNPs and fucoidan-stabilized AuNPs for 24 hours. After that, the serum-free media in each well were collected, centrifuged to remove cell debris, and kept at -80°C until use. The gelatin zymography was carried out on the collecting media using gelatin-incorporated SDS-polyacrylamide gel electrophoresis (7.5% SDS-polyacrylamide gel containing 1 mg/ml of gelatin). After electrophoresis, the gels were washed twice with 2.5% Triton X-100 for an hour to remove SDS, and incubated for 24 hours at 37°C with incubation buffer (50 mM of Tris-HCl, pH 7.5 containing 5 mM of $CaCl_2$, 1 µM of $ZnCl_2$, and 0.05% of

NaN_3). Then, the gels were stained with 0.3% coomassie brillilant blue in 30% methanol and 10% acetic acid, and de-stained with 30% methanol and 10% acetic acid. The bands of MMPs were visualized as clear bands on the blue background and the appearing bands were compared with a band of standard molecular weight marker which the molecular weights of MMP-2 and MMP-9 are 72 kDa and 92 kDa, respectively.

2.5 Statistical analysis

Cell viability and inhibitory effects of AuNPs were expressed as average ± S.D. (n=3) and statistically significant difference was determined with Student's t-test; p-value ≤ 0.05.

CHAPTER IV

RESULTS AND DISCUSSION

1. Preparation of fucoidan-stabilized gold nanoparticles

To find out the suitable preparation of AuNPs, the weight ratios of gold (Au) to fucoidans were varied from; 1:5, 1:10, 1:20, 1:30, 1:40, 1:50 to 1:60. As shown in Figures 10 and 11, obtained fucoidan-stabilized AuNPs were determined by visual observation for their separation after preparation and one month storage. AuNPs stabilized by algal fucoidans, OM and TK fucoidans, appeared to be pink to red-purple solution indicating that the nano-scaled gold particles were formed. No separation was visualized after synthesis and over one month storage for both fucoidan-stabilized AuNPs.

Surface plasmon resonance (SPR) of fucoidan-stabilized AuNPs was determined using UV-Vis spectroscopy. The peaks of optical spectra of AuNPs are usually present at the wavelength of around 520-540 nm (Likhatskii and Mikhlin, 2007). Moreover, the maximum wavelengths (λ_{max}) of SPR spectra depend on size and shape of AuNPs in which the wavelengths are shifted longer due to an increase of particle diameter (Jain *et al.*, 2007). According to UV-Vis spectroscopy results, the maximum wavelengths (λ_{max}) of both fucoidan-stabilized AuNPs were in the range of 515-550 nm, indicating that there were AuNPs present in the colloidal solution (Table 1). The obtained optical spectra showed that at 1:20 and 1:50 ratios of Au to algal fucoidans provided the highest absorbance peaks for OM-AuNPs and TK-AuNPs, respectively (Figure 12). Hence, 1:20 and 1:50 were optimum ratios for AuNP synthesis by using OM fucoidan and TK fucoidan, respectively, and were used for further experiments.

(A)

(B)

Figure 10 Appearance of OM-AuNPs in varying weight ratios of Au to OM fucoidan; 1:5, 1:10, 1:20, 1:30, 1:40, 1:50 and 1:60 (from left to right) after synthesis (A) and one month storage (B)

(A)

(B)

Figure 11 Appearance of TK-AuNPs in varying weight ratios of Au to TK fucoidan; 1:5, 1:10, 1:20, 1:30, 1:40, 1:50 and 1:60 (from left to right) after synthesis (A) and one month storage (B)

Table 1 UV peak absorption wavelength (λ_{max}) of algal fucoidan-stabilized AuNPs at various weight ratios of Au to fucoidan

The weight ratio of Au : fucoidan	OM-AuNPs		TK-AuNPs	
	λ_{max} (nm)	Absorbance	λ (nm)	Absorbance
1 : 5	530.0	0.344	547.5	0.216
1 : 10	529.0	0.353	543.5	0.262
1 : 20	527.0	0.387	537.0	0.320
1 : 30	523.5	0.380	534.5	0.326
1 : 40	521.0	0.377	529.0	0.317
1 : 50	521.0	0.377	529.5	0.382
1 : 60	518.5	0.368	522.0	0.321

Fucoidan-stabilized AuNPs prepared at room temperature (RT) have been investigated using the optimum ratios of Au to fucoidan obtained earlier. The experiment followed Singaravelu and colleagues who successfully prepared AuNPs using marine alga, *Sargassum wightii* Greville (Singaravelu *et al.*, 2007). The AuNP synthesis was performed under stirring condition at RT until the unchanged surface plasmon resonances were observed. During the reactions, spectra of the AuNPs were measured and the results showed that the absorbance peaks of the spectra are increased by time and became plateau after 48 hours of reaction (Figure 13). The finding indicated that fucoidan-stabilized AuNPs could be prepared without heating however this method has taken long period of time. Thus, heat-accelerated synthesis was performed in further experiments.

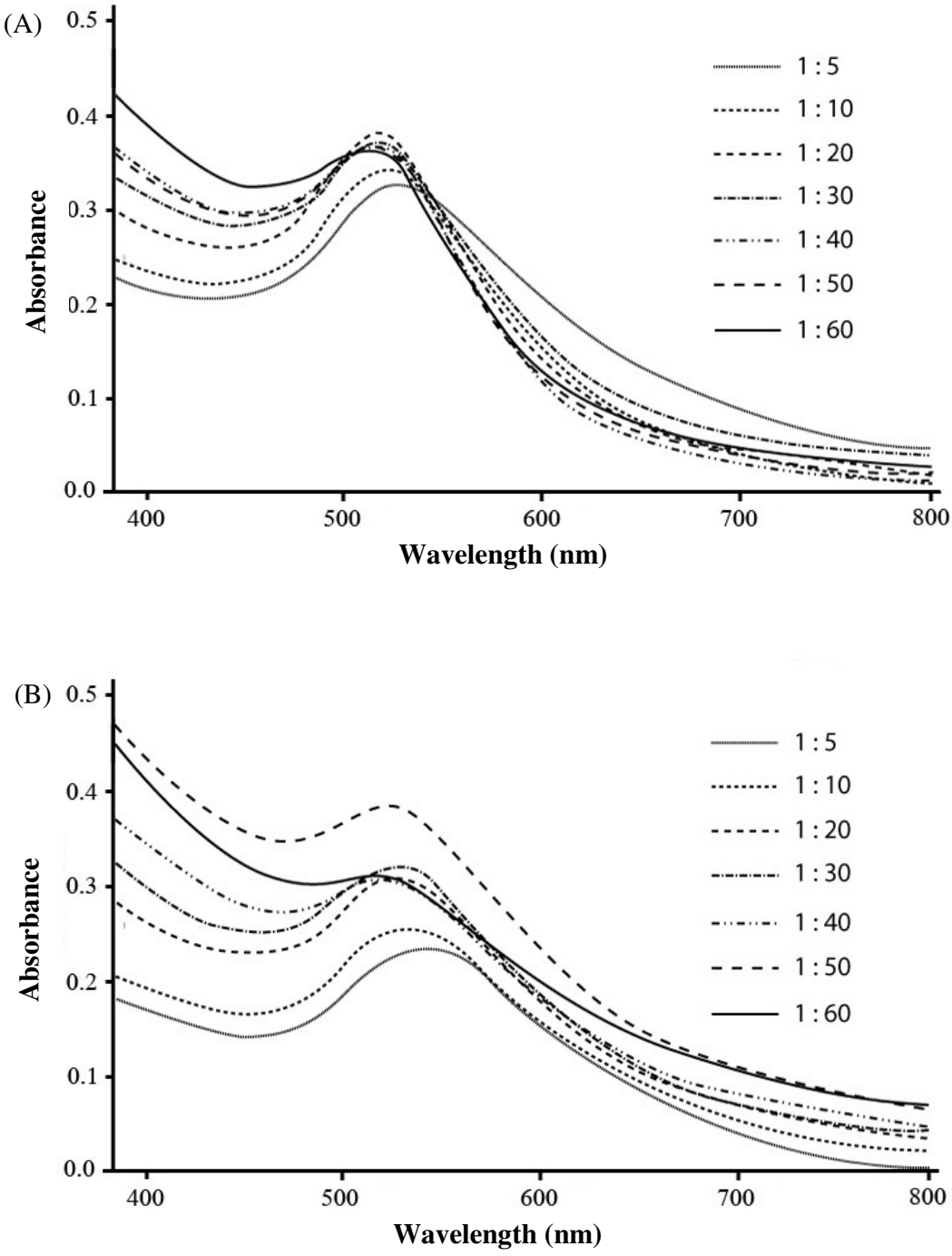

Figure 12 UV-Vis spectra of fucoidan-stabilized AuNPs at varying weight ratios of Au to OM fucoidan (A) and TK fucoidan (B)

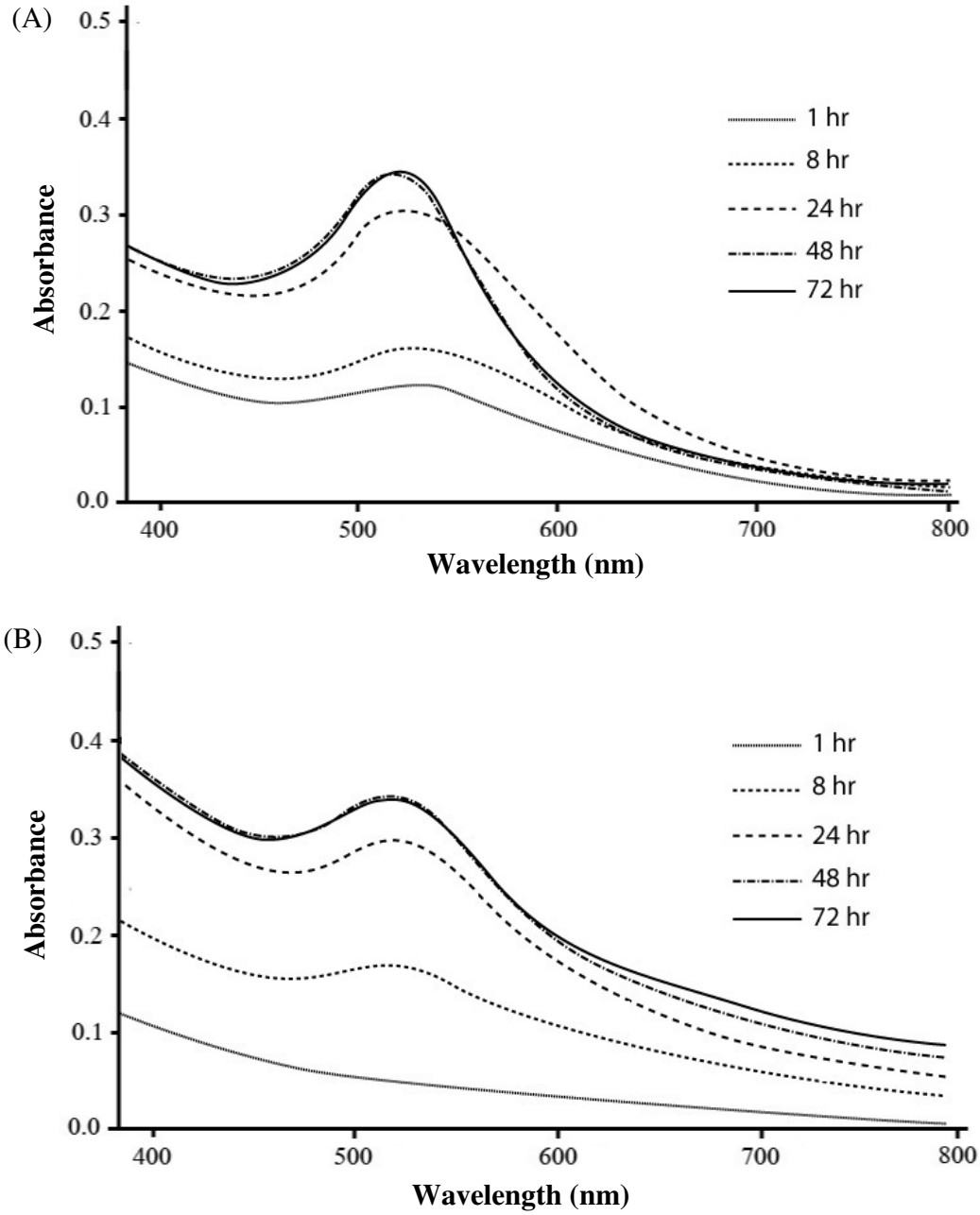

Figure 13 UV-Vis spectra of fucoidan-stabilized AuNPs prepared at RT; OM-AuNPs (A) and TK-AuNPs (B)

2. Characterization of fucoidan-stabilized gold nanoparticles

UV-Vis spectroscopy was used to determine SPR of fucoidan-stabilized AuNPs, the appropriate ratios of OM-AuNPs and TK-AuNPs have been investigated. According to UV-Vis spectra results, the peaks of both fucoidan-stabilized AuNPs were present in the similar wavelength (527.0 nm and 529.0 nm of OM-AuNPs and TK-AuNPs, respectively). However, the spectrum of OM-AuNPs was narrower than the spectrum of TK-AuNPs suggesting that AuNPs stabilized by TK fucoidan were broader in size distribution than OM-AuNPs (Figure 14).

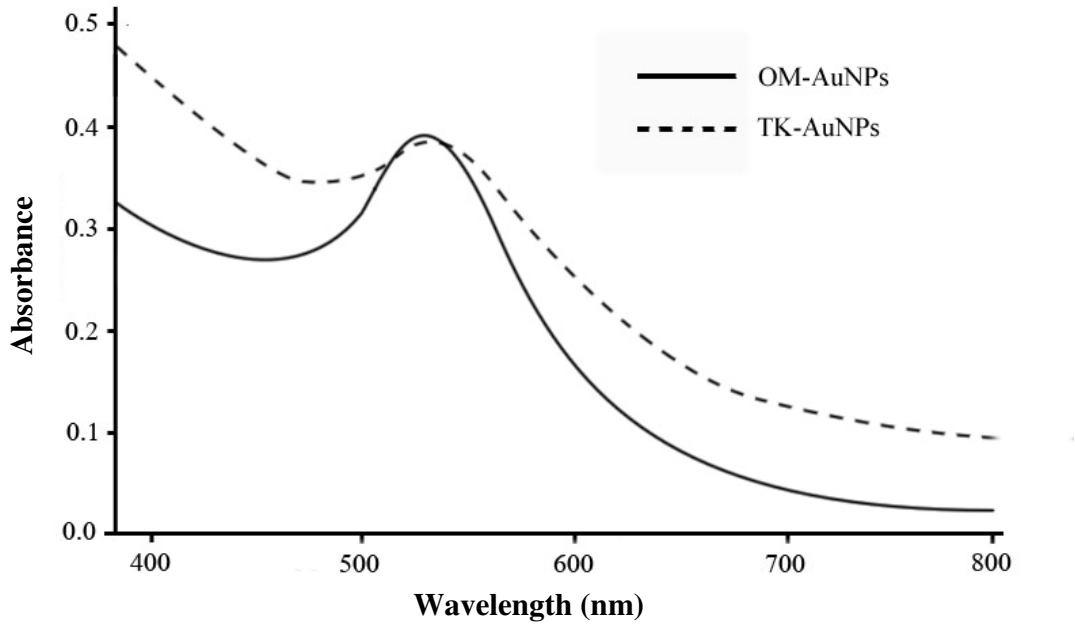

Figure 14 UV-Vis spectra of OM-AuNPs and TK-AuNPs prepared using the appropriate ratios of 1:20 and 1:50 Au to fucoidan, respectively.

Moreover, SPR bands of fucoidan-stabilized AuNPs were determined after synthesis and one month storage. The results indicated that unchanged spectra of AuNPs were obtained after one month storage (Figure 15). Therefore, fucoidan-stabilized nanoparticles seemed to be stable after one month storage.

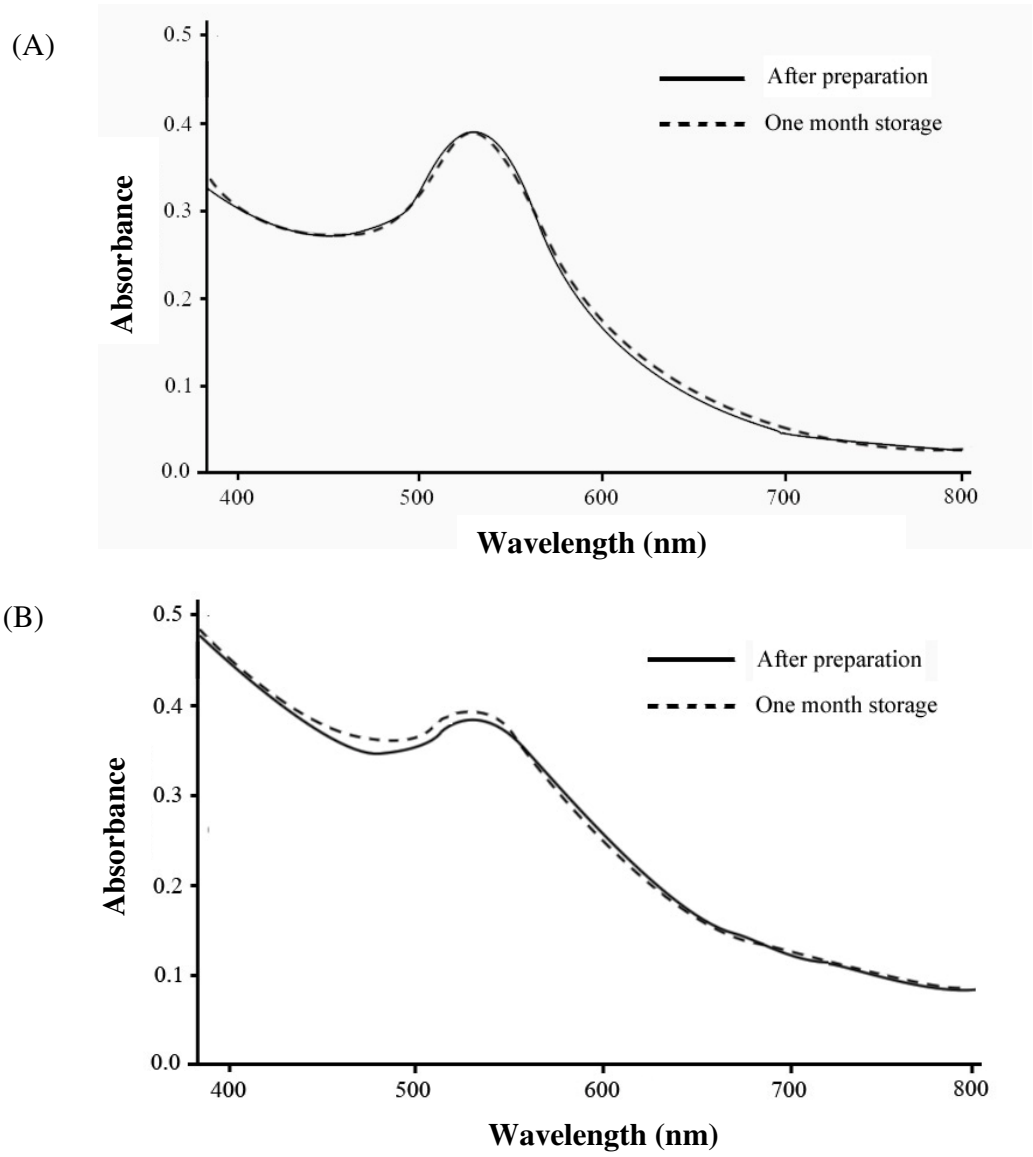

Figure 15 UV-Vis spectra of fucoidan-stabilized AuNPs after preparation and one month storage, OM-AuNPs (ratio of 1:20) (A) and TK-AuNPs (ratio of 1:50) (B)

Zeta potential of nanoparticles generally indicates the surface charge property of the nanoparticles which depends on the particle composition and the dispersed medium. Furthermore, nanoparticles with a zeta potential above ±30 mV (absolute value) have been found in stable colloidal nanoparticles due to electrostatic repulsion of the surface charge preventing particles from an aggregation (Singh and Lillard, 2009). The results revealed that surface charges of both fucoidan-stabilized AuNPs were in negative values indicating that particles were stabilized by negatively charged sulphate groups which were abundant in fucoidan structures. As shown in Table 2, zeta potential of AuNPs stabilized by OM fucoidan was more than -30 mV implying that OM-AuNPs were stable. In comparison, zeta potential obtained from TK-AuNPs was less; however, the value was still not far from -30 mV. In addition, zeta potential of OM-AuNPs remained unchanged whereas zeta potential of TK-AuNPs was slightly increased after storage (Table 2).

Table 2 Zeta potential of fucoidan-stabilized AuNPs

Type of AuNPs	Zeta potential (mV) ± S.D. (n = 3)	
	After synthesis	One month storage
TK-AuNPs	-21.72 ± 1.31	-27.01 ± 1.83
OM-AuNPs	-37.77 ± 4.83	-37.62 ± 3.34

TEM images of freshly prepared fucoidan-stabilized AuNPs were examined. AuNPs stabilized by OM fucoidan and TK fucoidan were shown to be spherical in shape. The particle distribution of OM-AuNPs was more mono-dispersed compared to TK-AuNPs (Figures 16A and 17A). The average size of OM-AuNPs was 8.54 ± 2.96 nm (n=564) and of TK-AuNPs was 10.74 ± 4.78 nm (n=422). The histogram of the size distribution indicated that TK-AuNPs had more size deviation than OM-AuNPs (Figures 16C and 17C). The finding was in agreement with the earlier results in that the broader absorbance spectra of TK-AuNPs than that of OM-AuNPs (Figure 14). Moreover, it was noted that the EDS spectrum was used to confirm that the observed nanoparticles were AuNPs in which the particles mainly contained Au element (Appendix A).

OM-AuNPs were still spherical and well distributed over one month storage whereas TK-AuNPs turned into variable in shape and coalescence (Figures 16B and 17B). After one month storage, the average size of OM-AuNPs remained similar to the size after synthesis (8.35 ± 2.83 nm, n=233) whereas larger particle sizes were obtained for TK-AuNPs (57.98 ± 13.89 nm, n=52). The results showed that OM-AuNPs were more stable than TK-AuNPs after 1-month storage were in consistent with the former results from zeta potential measurement.

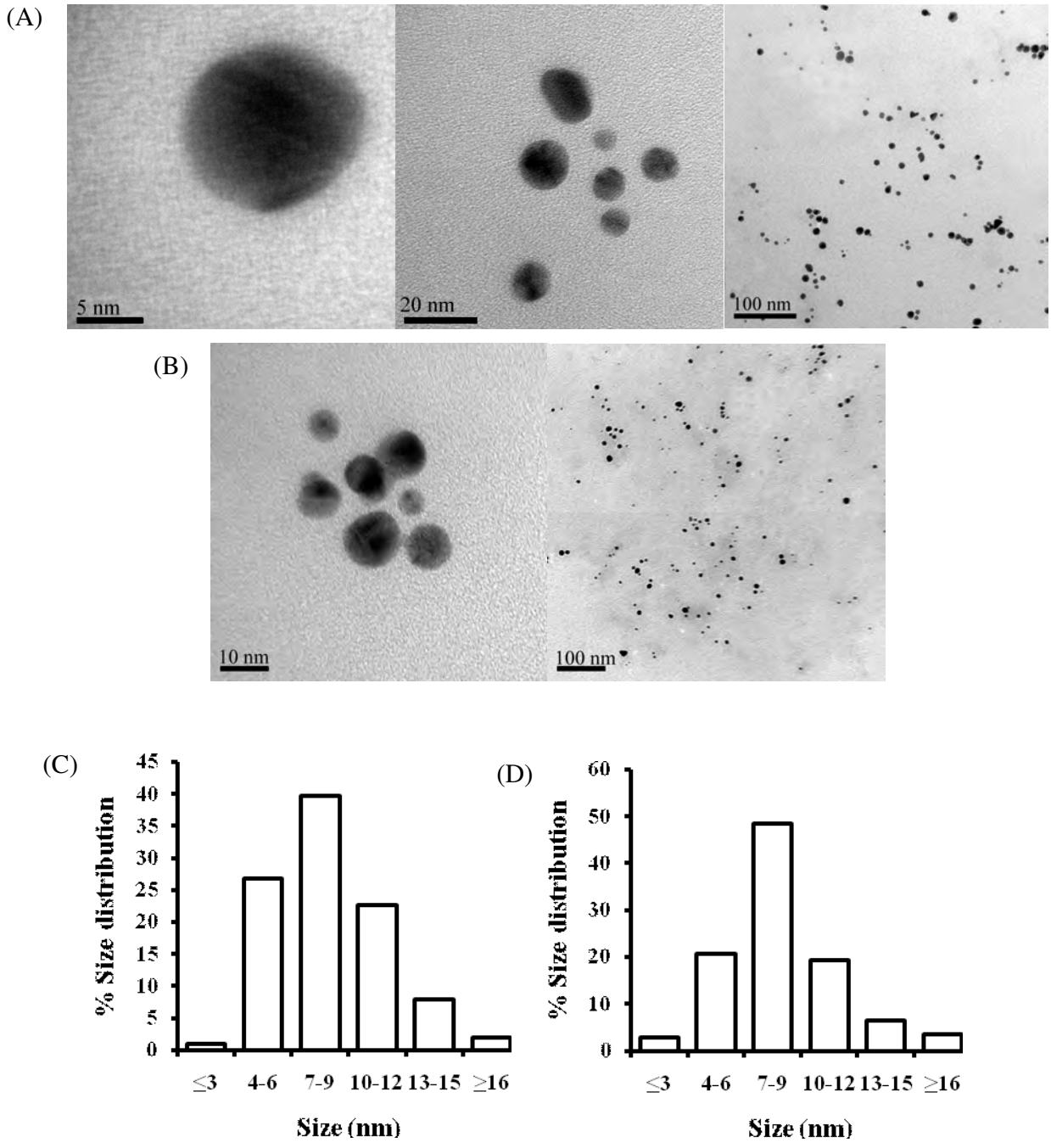

Figure 16 TEM images of OM-AuNPs after synthesis (A) and one month storage (B). Histogram of particle size distribution of OM-AuNPs after synthesis (C) and one month storage (D)

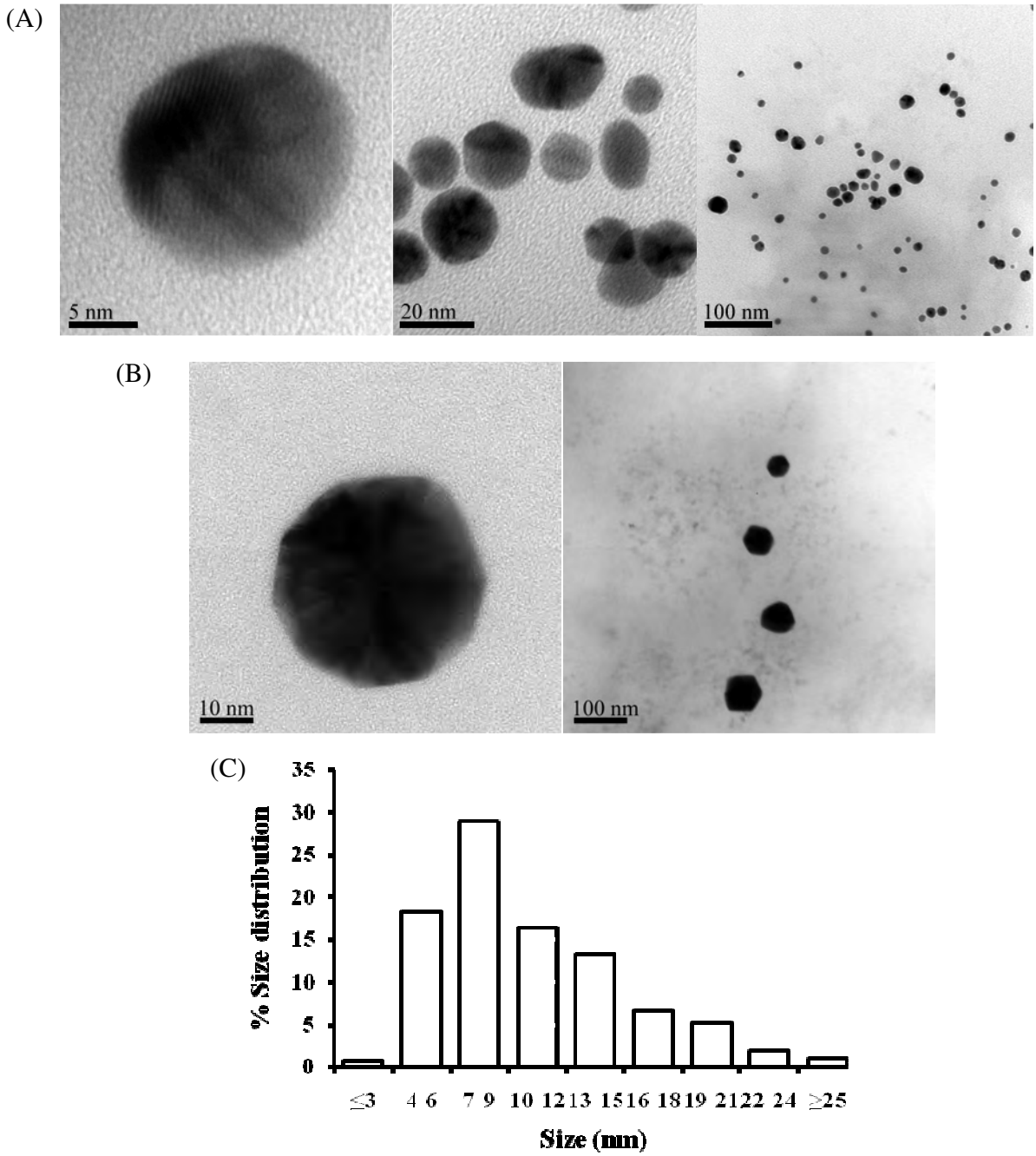

Figure 17 TEM images of TK-AuNPs after synthesis (A) and one month storage (B). Histogram of particle size distribution of TK-AuNPs after synthesis (C)

With rapid development of nanotechnology, green synthesis of the nanoparticles has to be concerned for safety and environmental benefits (Huang *et al.*, 2004; Sun *et al.*, 2008). This report successfully synthesized AuNPs by green method using natural agents, fucoidans, as reducing and stabilizing agents. AuNPs stabilized by OM fucoidan were mono-dispersed and stable for at least a month. However, AuNPs stabilized by TK fucoidan showed broader in particle distribution and become less stable after one month. The difference in ability to stabilize AuNPs might be due to the variation in fucoidan structures obtained from two different species of marine brown algae. Apart from electrostatic repulsive force of OM-AuNPs and TK-AuNPs, OM fucoidan mostly contains sulphated L-fucose polysaccharide with a few of short side chains which may have steric effect preventing the AuNPs from an aggregation by polymer stabilization. On the other hand, TK fucoidan contains structures with long and many side chains which could possibly cause inter-particle interaction and might lead to poor particle distribution and finally aggregation of the nanoparticles.

3. Estimation of fucoidan amount in the colloidal gold nanoparticles

To estimate the quantity of fucoidan associated with AuNPs, the complex of algal polysaccharide and methylene blue was determined using UV-Vis spectroscopy. The spectra of dye alone normally exhibit the peak around 664 nm and the absorbance at the peak is decreased after complex formation with polysaccharide (Jiao and Liu, 1999). In this study, known amount of sulphated polysaccharide (fucoidan) in the concentration range of 0-3 µg/ml was used for calibration. The diluted supernatant obtained from ultracentrifugation of 2 mM (0.4 mg/ml) fucoidan-stabilized AuNPs which contained 8

mg/ml or 20 mg/ml of OM fucoidan or TK fucoidan, respectively. A decrease in the peak absorbance due to fucoidan-dye complex was then calculated as free stabilizer and the amount of fucoidan fabricating the AuNPs was obtained. The results revealed that amounts of fucoidan in OM-AuNPs was 2.81 ± 0.42 mg/ml (~35.13 %conjugation) and in TK-AuNPs was 6.63 ± 0.69 mg/ml (~33.15 %conjugation).

4. Anti-tumor tests of fucoidan-stabilized gold nanoparticles

4.1 Cytotoxic effect of fucoidan-stabilized AuNPs on A549 cells in anchorage-dependent condition

MTT assay was used to investigate whether fucoidan-stabilized AuNPs have the ability to reduce viability of A549 cells. In this study, A549 cells were allowed to attach to a 96-well plate overnight before incubation with the samples for one day and three days. According to the results of 24-hour treatment, OM fucoidan decreased A549 cell viability more than TK fucoidan but the cytotoxic effect on A549 cells of TK-AuNPs was similar to OM-AuNPs (Figure 18). Expectedly, 3-day treatment with fucoidans resulted in more reduction of cell viability compared to 1-day treatment and the cytotoxic effect was in a dose-dependent manner for both of fucoidans. OM fucoidan had slightly more toxicity than TK fucoidan and OM-AuNPs had more cytotoxic effect than TK-AuNPs (Figure 19). The cytotoxic effect of Cit-AuNPs was also investigated and no significance of toxicity was found on A549 cells (in that the viability was more than 95%). In comparison, fucoidan-stabilized AuNPs significantly resulted in more cancer cell death than the corresponding fucoidans for all treatments with the exception of OM-AuNPs, 1-day treatment at 100 µg/ml (Figures 18 and 19).

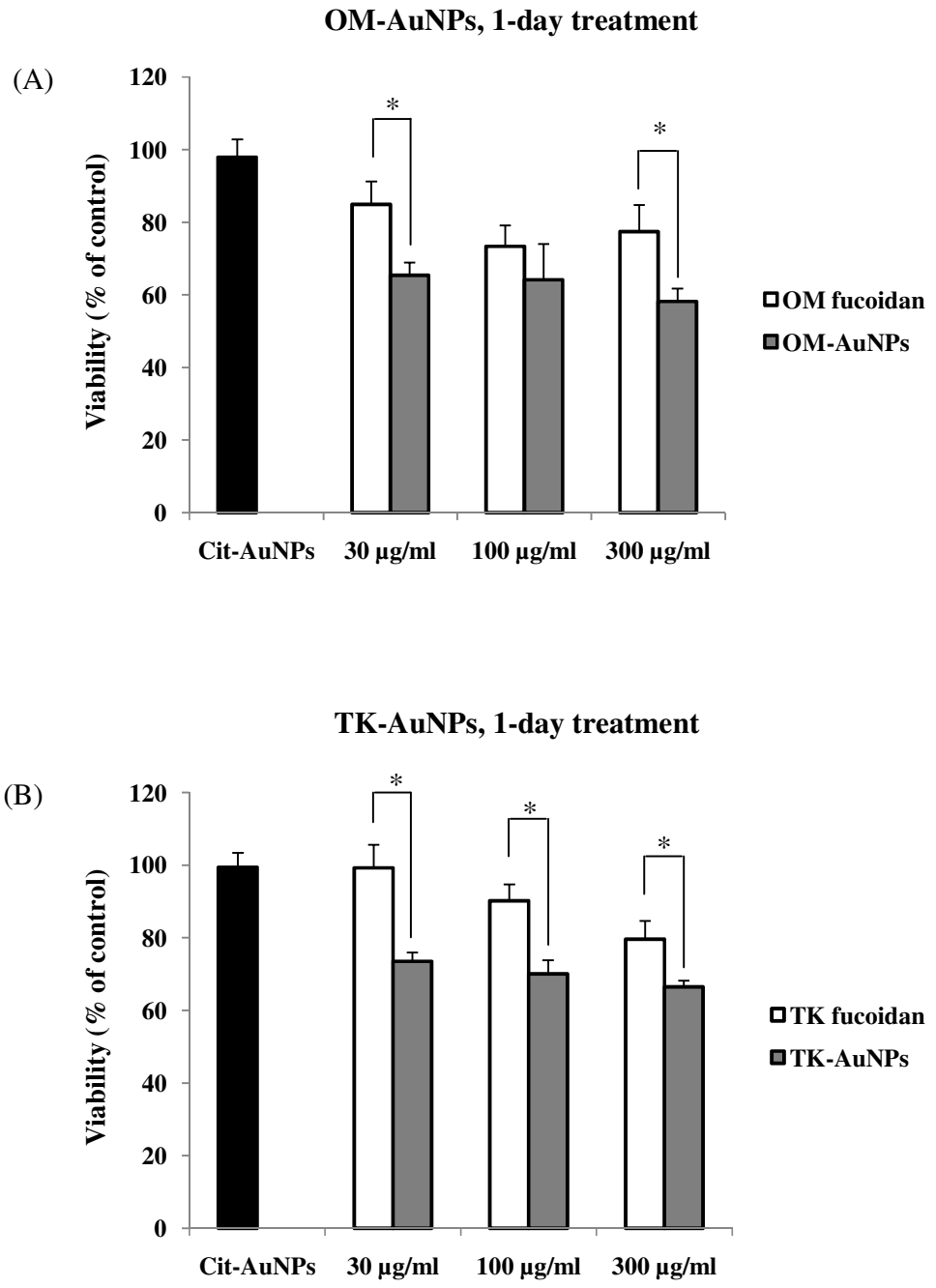

Figure 18 Percentage of viability of A549 cells after 1-day treatment with Cit-AuNPs, OM fucoidans and OM-AuNPs (A), TK fucoidan and TK-AuNPs (B) (n=3). * are significant differences at $p \leq 0.05$ of AuNPs compared to solely fucoidan.

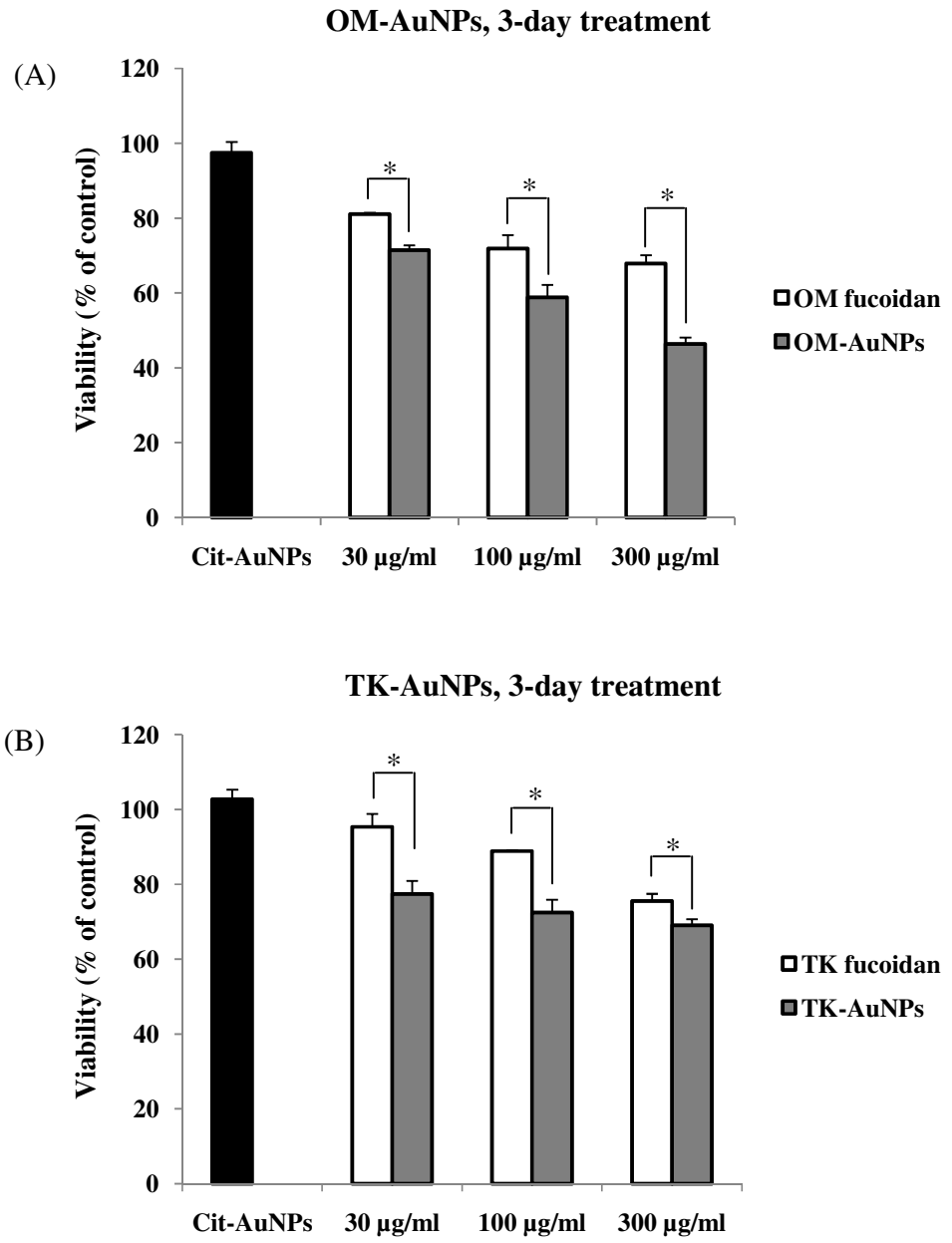

Figure 19 Percentage of viability of A549 cells after 3-day treatment with Cit-AuNPs, OM fucoidans and, OM-AuNPs (A), TK fucoidan and TK-AuNPs (B) (n=3). * are significant differences at $p \leq 0.05$ of AuNPs compared to solely fucoidan.

Cytotoxicity of algal fucoidans was reported in some cell lines; fucoidan from *Cladosiphon okamuranus* had a weak anti-proliferative effect (more than 80% cell viability) on human leukemia (U397) cell line when incubated with 100 µg/ml of fucoidan for three days (Teruya *et al.*, 2007). When 0-500 µg/ml of fucoidan from *C. okamuranus* was used, there was no cytotoxic effect (more than 80% cell viability) on human T-cell leukemia virus (HTLV-1)-infected T-cell line but there was an effect at the higher doses up to 3,000 µg/ml (Haneji *et al.,* 2005). On the other hand, after four days of treatment with 1,000 µg/ml fucoidan from *C. okamuranus*, growth inhibition on stomach cancer cell line (MKN45) (about 40% cell growth) was observed (Kawamoto *et al.*, 2006). There was no previous report on cytotoxic effect of fucoidan obtained from *K. crassifolia* (TK fucoidan) used in this study. However, fucoidan from *Laminaria guryanovae* which belongs to the same order of TK fucoidan (Laminariales) had no toxic effect (~80% cell viability) on mouse epidermal (JB6 Cl41) cells after 3-day incubation with 200 µg/ml fucoidan (Lee *et al.*, 2008). According to the cytotoxic results, weak growth inhibitory effect was observed after 1-day or 3-day treatment of A549 cells with 30, 100 and 300 µg/ml OM fucoidan (81, 71.9 and 67.8% cell viability) and TK fucoidan (95.3, 88.9 and 75.5% cell viability). These results agreed with previous reports in which fucoidans had a slight cytotoxic effect on cell lines at the lower doses and the toxicity might increase at the higher dose of algal fucoidan (Haneji *et al.,* 2005).

For Cit-AuNPs, the nanoparticles did not present a toxic effect on A549 cell line. The results were in consistent with previous reports in that Cit-AuNPs were comparatively non-toxic on other cell lines. For examples, at 300 µM Cit-AuNPs did not cause cytotoxic effect on human dermal fibroblasts-fetal (HDF-f) cells (Qu and Lu, 2009)

and no cytotoxicity was observed on leukemia cell line (K562) after treatment with 250 μM Cit-AuNPs (Lewinski, Colvin and Drezek, 2008).

According to the fucoidan-stabilized AuNPs cytotoxic results, OM-AuNPs and TK-AuNPs were significantly higher in cytotoxicity than their corresponding fucoidans which might be possibly due to the improved cellular penetration of fucoidans-stabilized AuNPs. Some reports revealed that conjugation of drugs with AuNPs could enhance potency and delivery to target sites. Hosta and coworkers (2009) reported that kahalalide F conjugated with AuNPs improved the delivery of drug to the target cells (Hosta *et al.*, 2009), while insulin conjugated with chitosan-AuNPs promoted the penetration and uptake of the peptide hormone for transmucosal delivery (Bhumkar *et al.*, 2007). Tamoxifen conjugated with AuNPs were able to enhance drug potency owing to more intracellular drug transport *via* nanoparticle endocytosis than passive diffusion of free drug in *in vitro* (Dreaden *et al.*, 2009).

4.2 Cytotoxic effect of fucoidan-stabilized AuNPs on A549 cells in anchorage-independent condition

Anoikis resistance relates to survival ability of cancer cells during the condition of detachment which is concerned to be a critical step of metastasis. Therefore, this part of study was aim to determine the cytotoxic effect of fucoidan-stabilized AuNPs in detached A549 cells. Poly-HEMA was used to avoid the cell attachment to 96-well plate in which the cells formed aggregate after incubation (Appendix C). For 1-day treatment, there was not much difference in cytotoxic effect on detached A549 cells between OM fucoidan and TK fucoidan as well as cytotoxic effect between OM-AuNPs and TK-AuNPs (Figure 20). After 3-day treatment, OM fucoidan could decrease A549 cell viability more than

TK fucoidan and the cytotoxic effect of OM-AuNPs was more than that of TK-AuNPs (Figure 21). While, Cit-AuNPs had no any cytotoxic effect on detached A549 cells for both one day and three days of treatment. The results indicated that the effect of fucoidan-stabilized AuNPs was not different from the corresponding fucoidans.

For anchorage-independent condition, A549 cells responded similarly to both fucoidan-stabilized AuNPs regardless of the types of fucoidan. AuNPs had the same effect on A549 cells as their corresponding fucoidans in anchorage-independent condition while the AuNPs were more toxicity in anchorage-dependent condition. The different results might be due to the aggregation of A549 cells after incubation in poly-HEMA coated 96-well plates used in anchorage-independent condition. There was some report on hepatoma cells (BEL7402) aggregation formation mediated anoikis resistance (Zhang *et al*., 2008). The cancer cell were attached and self-assembled into aggregation to compensate the lacking of ECM attachment. Then, the cancer cell aggregations led to an increase in size and the cells at surface of aggregation were formed to become molecular barriers. These barriers caused the aggregation to resist to outside stimuli and protected cells in the center of the aggregation. Therefore, the AuNPs might not pass easily through the A549 cell aggregations to affect the entire cell colony in anchorage-independent condition.

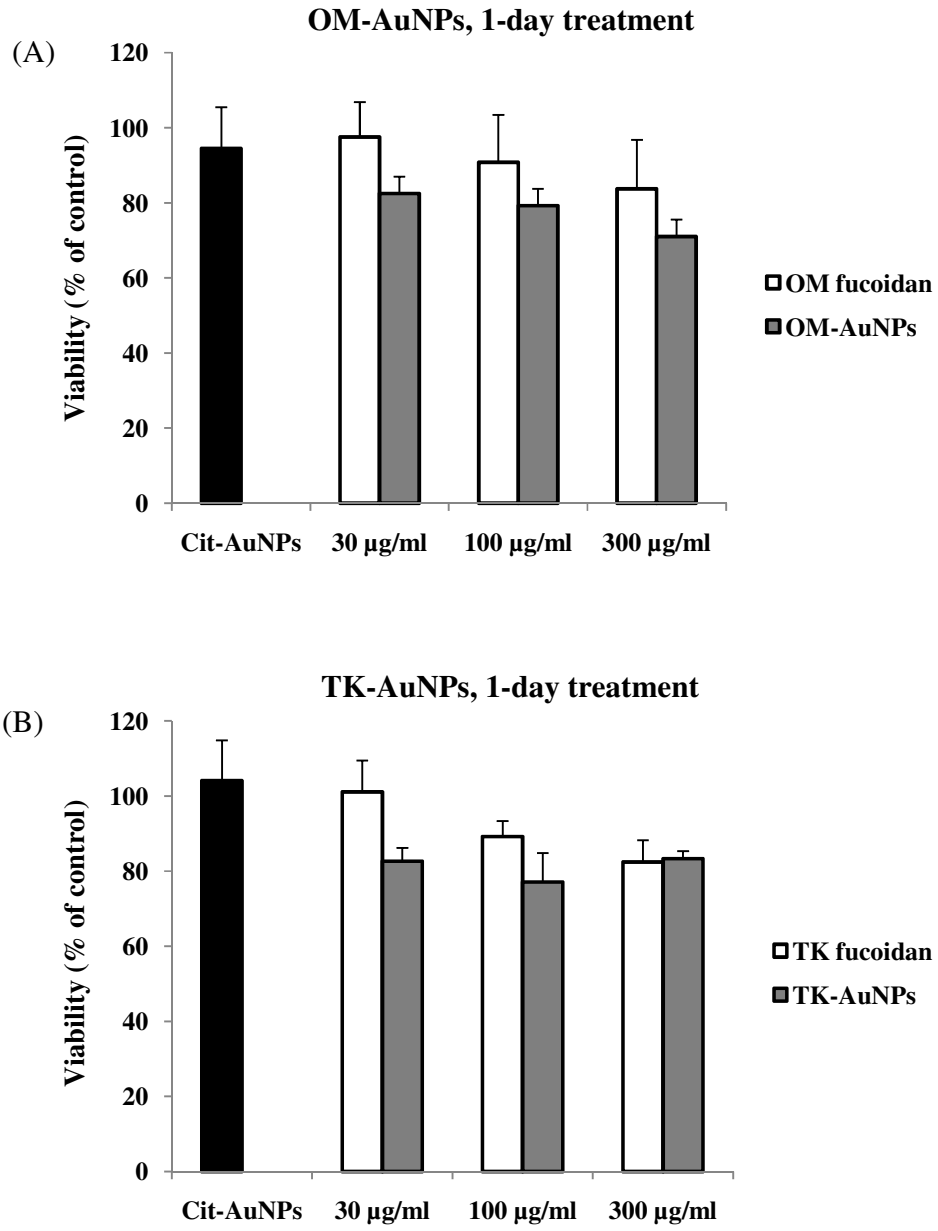

Figure 20 Percentage of viability of detached A549 cells after 1-day treatment with Cit-AuNPs, OM fucoidans and OM-AuNPs (A), TK fucoidan and TK-AuNPs (B) (n=3).

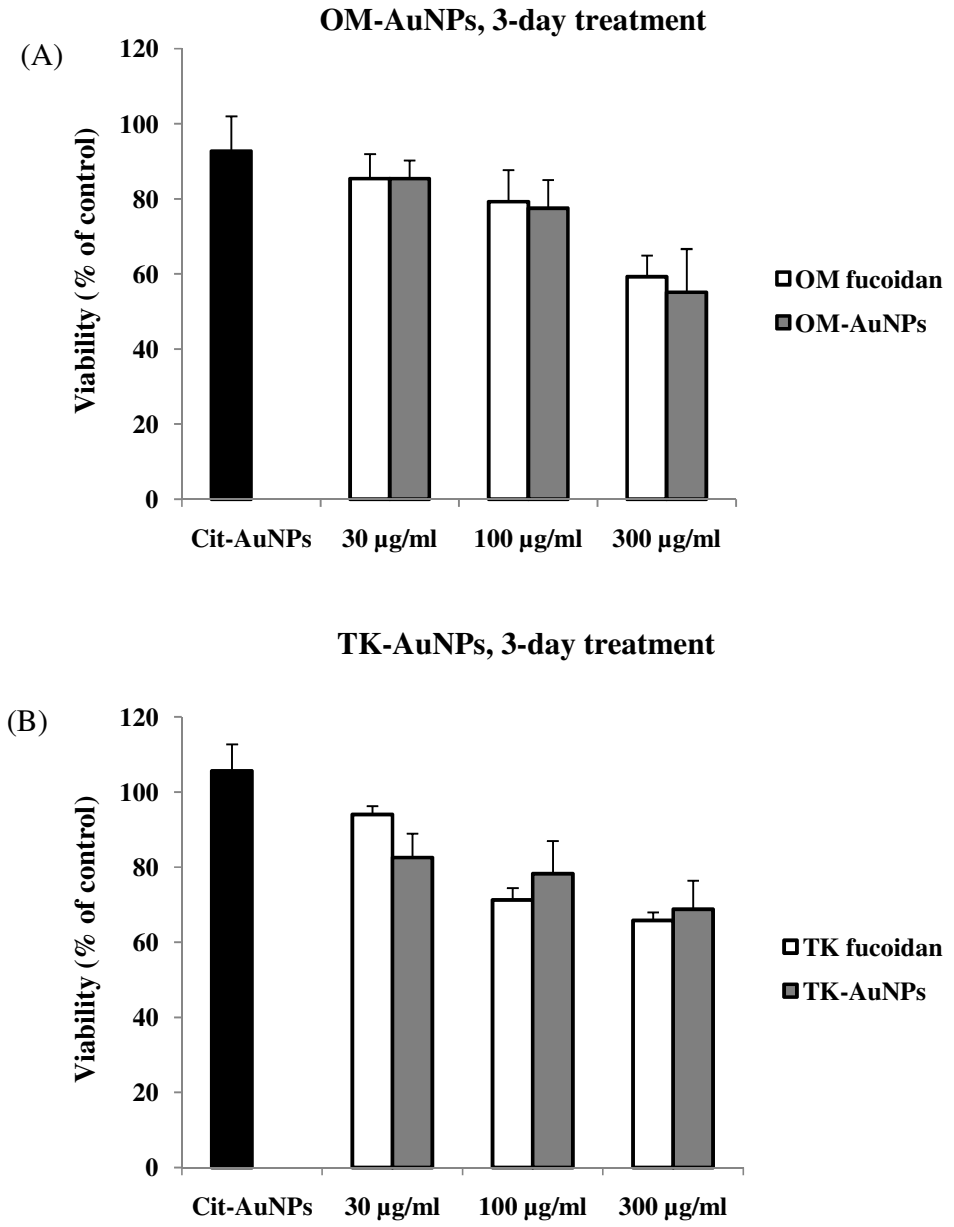

Figure 21 Percentage of viability of detached A549 cells after 3-day treatment with Cit-AuNPs, OM fucoidans and OM-AuNPs (A) and TK fucoidan and TK-AuNPs (B) (n=3).

In addition, two standard anti-cancer drugs, 0.1 µg/ml of paclitaxel and 1 µg/ml of etoposide, were tested for cytotoxic effect in both anchorage-dependent (attached cells) and anchorage-independent conditions (detached cells) on A549 cell line. Interestingly, A549 cells were resistant to paclitaxel in anchorage-independent condition, as shown in Figure 22, the viability of detached A549 cells after three days of treatment with paclitaxel (~70% cell viability) was significantly more than viability of attached A549 cells (~30% cell viability). On the other hand, the viability of etoposide-treated A549 cells was similar in both attached and detached cells. Likewise, A549 cells seemed irresistible to fucoidans and fucoidan-stabilized AuNPs in anchorage-independent condition. In comparison, at the highest dose of fucoidan used (300 µg/ml), no significant differences in viability of A549 cells were observed when treated with fucoidans and fucoidan-stabilized AuNPs with the exception of TK-AuNPs, 1-day treatment. For an anchorage-dependent condition, OM-AuNPs and TK-AuNPs decreased A549 cell viability. However, the toxicity of AuNPs was not potent (~45% and ~70% cell viability for OM-AuNPs and TK-AuNPs, respectively after 3-day treatment) as the toxicity of paclitaxel (~30% cell viability) (Figure 22).

The finding revealed that detached A549 cells were resistant to paclitaxel whereas no resistance was observed on etoposide treatment in the loss of attachment condition. There were some studies reported that anoikis resistance is associated with less sensitivity of several standard anti-cancer drugs. Frankel *et al*. (1997) revealed that many ovarian carcinoma cell lines, HEY, A2780, SKOV3 and OVCA 429 established the resistance toward paclitaxel while these cancer cell lines were not resistant to cisplatin. Kim *et al.*

(2010) reported that breast cancer cell lines, MDA-MB-231 and MCF-7 were resistant to the treatment of doxorubicin.

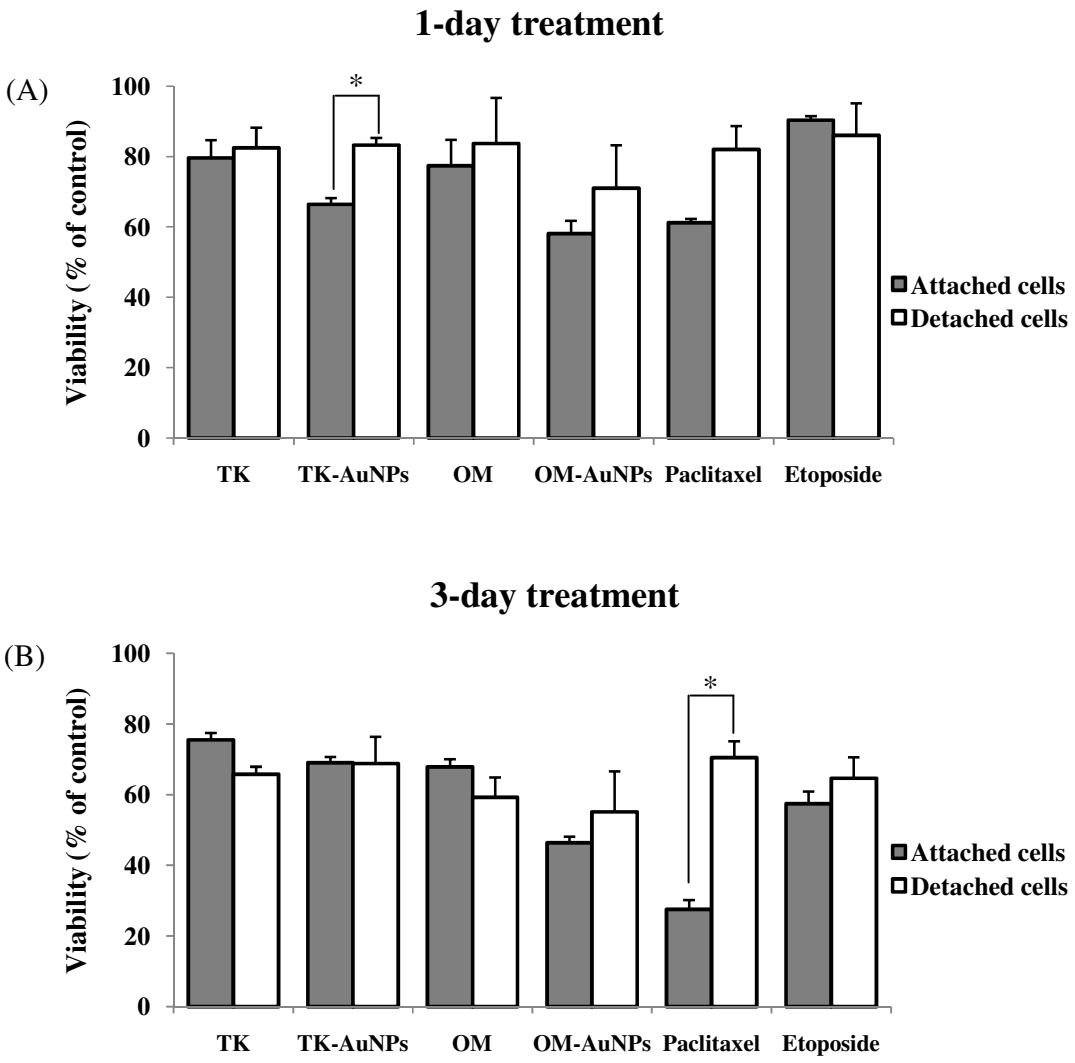

Figure 22 Percentage of viability of A549 cells after treatment with TK fucoidan, TK-AuNPs, OM fucoidan, OM-AuNPs (all at concentration of 300 µg/ml fucoidans), 0.1 µg/ml paclitaxel and 1 µg/ml etoposide, in anchorage-dependent and anchorage-independent conditions for one day (A) and three days (B) (n=3). * are significant differences at $p \leq 0.05$ of attached A549 cells compared to detached A549 cells.

According to the results, fucoidan-stabilized AuNPs decreased cell viability on detached A549 cells similarly to the results of attached A549 cells indicating that no resistance of A549 cells was found after treatment with the AuNPs. Therefore, fucoidan-stabilized AuNPs might be useful for prevention of cancer metastasis.

4.3 Inhibitory effect of fucoidan-stabilized AuNPs on A549 cell invasion

Invasion process is a sequential step which plays an important role to metastasis. In order to investigate the inhibitory effect of fucoidan-stabilized AuNPs on invasion of A549 cells, Transwell® attached with polycarbonate membrane filter was used in this experiment. The filter was pre-coated with cellular ECM, Matrigel®, to imitate the BM underlying epithelial cells. In this study, A549 cells had to attach and degrade Matrigel® followed by migrating toward the lower part of the filters which were induced by a chemoattractant, MRC-5 conditioned medium. The invading A549 cells attached with a lower part of Transwell® after incubation were quantified. In this study, fucoidan-stabilized AuNPs containing the highest concentration of preparable AuNPs, 300 µg/ml, were used. As shown in Figure 23, TK fucoidan and TK-AuNPs had no inhibitory effect while OM-AuNPs had a slight effect (84.82% invasion) similarly to OM fucoidan (88.64% invasion). Additionally, slight inhibitory effect on invasion of A549 cells was found after treatment with Cit-AuNPs (85.99% invasion). Hence, it seemed that TK fucoidan and TK-AuNPs had no inhibitory effect on A549 cell invasion. However, there was still no report on the relationship between types of fucoidan and the effect on invasion as well as a little known on the effect of fucoidan on cancer invasion. There was a report on enzyme-digested fucoidan extract from *C. novae-caledoniae kylin* which belongs to the same genus as OM fucoidan in that approximately 30% and 50% inhibition

on invasion of human fibrosarcoma cells (HT1080) were found after treatment with 1,100 and 2,200 µg/ml of fucoidan extract, respectively (Ye *et al*., 2005). However, the concentration of OM fucoidan used in this study was 300 µg/ml which considerately less than the previous experiment and might result in weakly inhibitory effect on A549 cell invasion.

Fucoidan from *F. vesiculosus* promoted invasion of human melanoma cells (MelJuso) at 100 µg/ml of fucoidan (Brunner *et al.*, 1998). On the other hand, the study of Seoda *et al*., (1994) revealed that this fucoidan inhibited about 50% invasion of Murine Lewis carcinoma (3LL) cells at the concentration of 10 µg/ml of fucoidan. Taken together, it can be concluded that the effect of fucoidan on invasion might depend on types of cell line and different species of marine brown algae which provide different complex fucoidan structures.

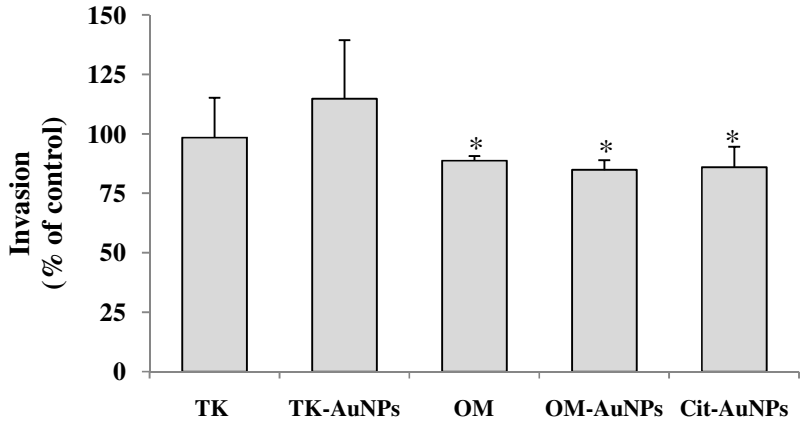

Figure 23 Percentage of invasion of A549 cells after 6-hour treatment with TK fucoidan, TK-AuNPs, OM fucoidan, OM-AuNPs (all at concentration of 300 µg/ml fucoidans) and Cit-AuNPs (n=3). * are significant differences at $p \leq 0.05$ compared to a control (medium).

4.4 Inhibitory effect of fucoidan-stabilized AuNPs on cell migration of A549 cells

Cell migration is one step in cancer invasion process and fucoidan-stabilized AuNPs were determined for cell migration of A549 cells. Cell migration was performed in the same way as invasion assay except for using the filter without ECM coated. Thus, A549 cells were able to move directly through the pores of the filter without any interaction of cells to ECM and the migrating A549 cells at a lower part of Transwell® after incubation were quantified. According to the results, TK and OM fucoidans, fucoidan-stabilized AuNPs and Cit- AuNPs did not decrease any migration of A549 cells (Figure 24).

Interestingly, fucoidans and fucoidan-stabilized AuNPs were found to promote an effect on A549 cell migration (Appendix F). Some previous studies suggested that fucoidan from *F. vesiculosus* stimulated the migration of HUVEC in the presence of VEGF165 (Lake *et al.*, 2006) and fibroblast growth factor (FGF)-1 but had a slightly inhibition on cell migration in the presence of FGF-2 (Giraux *et al.*, 1998). In contrast, fucoidan from *F. vesiculosus* showed the inhibitory effect on bFGF-induced cell migration of HUVEC with 50% inhibition at 10 µg/ml of fucoidan. Hence, inhibitory effect on cell migration of fucoidan might rely on inducing agents. For this cell migration assay, MRC-5 conditioned medium was used as a chemoattractant contained hepatocyte growth factor (HGF) which seemed to be responsible for supporting the cell migration (Stokel *et al.*, 1987). Therefore, fucoidans and fucoidan-stabilized AuNPs might potentiate A549 cell migration in the presence of HGF.

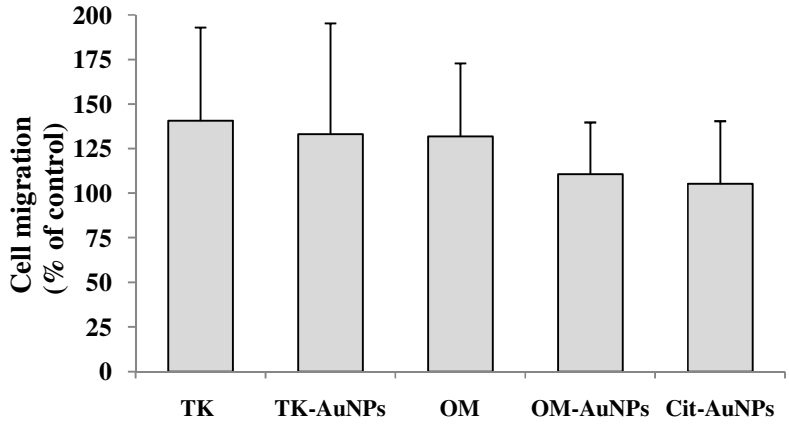

Figure 24 Percentage of cell migration of A549 cells (as compared to 100% of control) after 6-hour treatment with TK fucoidan, TK-AuNPs, OM fucoidan, OM-AuNPs (all at concentration of 300 µg/ml fucoidans) and Cit-AuNPs (n=3).

4.5 Inhibitory effect of fucoidan-stabilized AuNPs on adhesion of A549 cells

During invasion process, the cancer cells require adhesion to BM or ECM. Therefore, the inhibitory effect on adhesion of fucoidan-stabilized AuNPs was examined on A549 cell line. Cellular ECM or Matrigel® coated 96-well plates were used and the adherent cells after an hour of incubation were measured. From the results, no markedly inhibitory effect on adhesion was found among groups of test sample (Figure 25).

Moreover, the inhibitory effect on adhesion to fibronectin was also investigated on A549 cells. OM fucoidan and TK fucoidan showed a slightly inhibitory effect on adhesion of A549 cells to fibronectin (81.52% and 90.81% adhesion, respectively). The inhibitory effect of OM-AuNPs (73.46% adhesion) and TK-AuNPs (81.04% adhesion) were slightly more than fucoidans whereas no anti-adhesive effect to fibronectin was found on A549 cells after treatment with Cit-AuNPs (Figure 26).

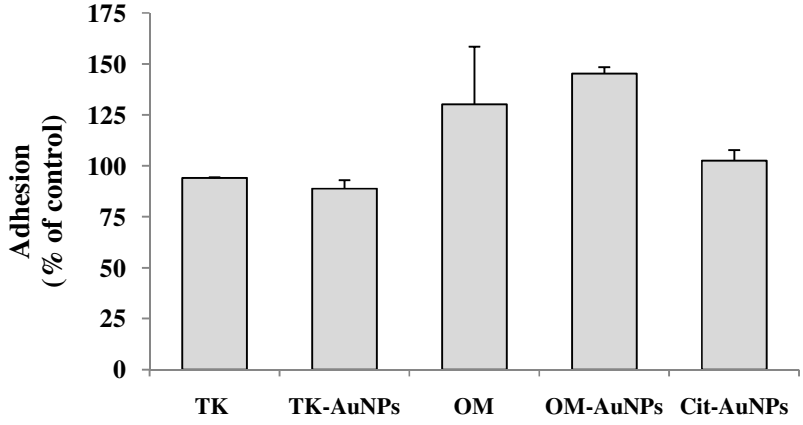

Figure 25 Percentage of adhesion of A549 cells to Matrigel® (compared to 100% of control) after 1-hour treatment with TK fucoidan, TK-AuNPs, OM fucoidan, OM-AuNPs (all at concentration of 300 µg/ml fucoidans) and Cit-AuNPs (n=3).

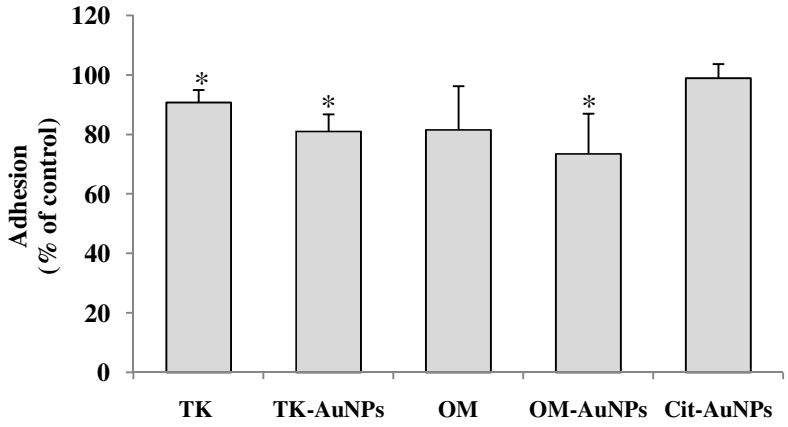

Figure 26 Percentage of Adhesion of A549 cells to fibronectin after 1-hour treatment with TK fucoidan, TK-AuNPs, OM fucoidan, OM-AuNPs (all at concentration of 300 µg/ml fucoidans) and Cit-AuNPs (n=3). * are significant differences at $p<0.05$ compared to a control (medium).

The results agreed with anti-adhesive property of other fucoidans reported previously. The effect of *A. nodosum* fucoidan on breast cancer cell line (MDA-MB-231) adhesion to fibronectin was studied and the results indicated that this fucoidan had anti-adhesive activities by ~20% and ~50% inhibition at 100 and 1,000 µg/ml fucoidan, respectively (Liu *et al*., 2005). Another study was reported on the effect of fucoidan from *S. schröederi* on wild-type Chinese hamster ovary cell (CHO-K1) adhesion to ECM protein including fibronectin, laminin, collagen type IV and vibronectin. The fucoidan inhibited cell adhesion to fibronectin and vibronectin on CHO-K1 (~20% inhibition at 100 µg/ml of fucoidan) whereas inhibitory effect was not present on the adhesion of cells to laminin and collagen type IV (Rocha *et al*., 2001). Moreover, fucoidan from *C. okamuranus* were reported on MDA-MB-231 adhesion to platelets and the result showed that at 100 µg/ml of this fucoidan did not significantly inhibit adhesion on this breast cancer cells to platelets (Cumashi *et al*., 2007).

4.6 Inhibitory effect of fucoidan-stabilized AuNPs on matrix metalloprotinases production in A549 cells

Matrix metalloprotinases (MMPs) are considerate to be important proteolytic enzymes for ECM remodeling step during cancer invasion, especially MMP-2 and MMP-9. From the gelatin zymography results, MMP-9 was not produced by A549 cells (data not shown) and the evaluation of MMP production was conducted on MMP-2 only. Gelatin zymography was quantified by Quantity One V.4.6.3 software (Biorad, USA) (Figure 27). It has been found that OM fucoidan inhibited MMP-2 production on A549 cells (~50% inhibition, at 300 µg/ml of fucoidan) while the inhibitory effect of OM-AuNPs was slightly more than the inhibitory effect (~60% inhibition) of OM fucoidan.

However, TK fucoidan had no significantly inhibitory effect on MMP-2 production of A549 cells whereas TK-AuNP had more inhibitory effect. Additionally, Cit-AuNPs did not show any inhibitory effect on MMP-2 production of A549 cells.

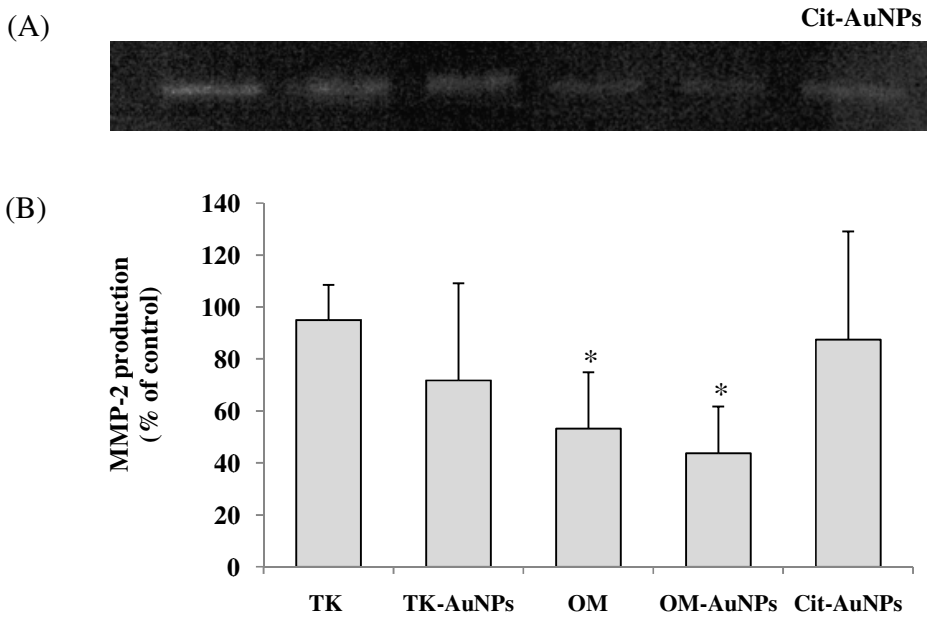

Figure 27 Zymogram of fucoidan-stabilized AuNPs on MMP-2 production in A549 cells after 24-hour treatment with a control (serum-free medium), TK fucoidan, TK-AuNPs, OM fucoidan, OM-AuNPs (all at 300 μg/ml fucoidan concentration) and Cit-AuNPs (A); Effect of fucoidan-stabilized AuNPs on MMP-2 production in A549 cells after 24-hour treatment with TK fucoidan, TK-AuNPs, OM fucoidan, OM-AuNPs (all at concentration of 300 μg/ml fucoidans) and Cit-AuNPs (B). * are significant differences at $p \leq 0.05$ compared to a control (serum-free medium).

According to the study of Senni *et al.* (2006), fucoidan from *A. nodosum* decreased MMP-2 in condition medium of human dermal fibroblast cells (35% and 45% decreased at 10 and 100 µg/ml of fucoidan, respectively). Ye *et al.* (2005) indicated that enzyme-digested fucoidan extracts from *C. novae-caledoniae kylin* inhibited MMP-2 production on HT1080 cells (~20% and 40% inhibition, at 1.1 and 2.2 mg/ml of fucoidan) suggesting that the down-regulation of MMP-2 might result in the inhibition of HT1080 cell invasion by fucoidan extract. Therefore, the capability of OM fucoidan to decrease A549 cell invasion would arise mainly by suppressing MMP-2 production.

In summary, fucoidan-stabilized AuNPs had a cytotoxic effect on A549 cells in both anchorage-dependent and anchorage-independent conditions. Interestingly, more toxicity of fucoidan-stabilized AuNPs than the toxicity of their corresponding fucoidans in anchorage-dependent condition was observed and A549 cells seemed not to resist to the treatment of fucoidan-stabilized AuNPs in anchorage-independent condition. OM-AuNPs presented a slight inhibition toward A549 cell invasion which might be due to anti-adhesive property to fibronectin and suppression of MMP-2 production of OM-AuNPs but no inhibitory effect of OM-AuNPs was found on cell migration. Although TK-AuNPs had a little inhibitory effect on A549 cell adhesion to fibronectin and slightly inhibitory effect on MMP-2 production but they did not show any inhibitory effect on A549 cell invasion.

CHAPTER V

CONCLUSION

AuNPs are attractive to be employed in many applications because they render many advantages including simplicity of AuNP synthesis, high stability and intense color of AuNPs providing specific optical properties. Surface modification of AuNPs has been used in medical area such as nano-sensor, imaging as well as for drug delivery approaches. Moreover, cancer therapy can be arisen from EPR effect and high cellular uptake of AuNPs due to the tiny size of the nanoparticles resulting in enhancement of drug efficacy and increasing the delivery of drugs to the target sites. In general, the synthesis of AuNPs involves synthetic chemical substances and organic solvents which bring about an increase in environmental toxicity and biological hazard. Therefore, preparation of AuNPs using natural compounds would provide an alternative method of AuNP synthesis.

This study successfully synthesized AuNPs by using fucoidan extracted from marine brown algae as reducing and stabilizing agents. In this study, OM fucoidan and TK fucoidan obtained from *Cladosiphon okamuranus* and *Kjellmaniella crassifolia*, respectively, were used for the AuNP synthesis. According to fucoidan-stabilized AuNP preparation, 1:20 and 1:50 were the appropriate weight ratios of Au to fucoidans for synthesis of OM-AuNPs and TK-AuNPs, respectively. The characterization of the AuNPs revealed that zeta potentials of the obtained AuNPs were -37.77 ± 4.83 and -21.72 ± 1.31 mV for OM-AuNPs and TK-AuNPs, respectively. Moreover, OM fucoidan could be stabilized AuNPs with mono-dispersion, well particle distribution (the average size = 8.54 ± 2.96 nm) and high stability superior than TK fucoidan (the average

size = 10.74 ± 4.78 nm). These might be due to the different structural features of fucoidans.

From the anti-tumor results, fucoidan-stabilized AuNPs (OM-AuNPs and TK-AuNPs) had a cytotoxic effect on human lung carcinoma (A549) cells and the toxic effects were greater than the effect of corresponding fucoidans in anchorage-dependent condition. This is possibly due to a enchaning effect between AuNPs and fucoidans, resulting in higher cellular uptake of fucoidans in the form of nanoparticles. Interestingly, after treatment with fucoidan-stabilized AuNPs in the condition of anchorage-independence, no A549 cell resistance was found, suggesting that fucoidan-stabilized AuNPs could be useful for metastasis prevention of cancer. Moreover, OM-AuNPs had a slight inhibition (~16% inhibition) on A549 cell invasion; this effect might come from their anti-adhesive property to fibronectin (~30% inhibition) and inhibition of MMP-2 production in A549 cells (~60% inhibition) of OM-AuNPs. Whereas, TK-AuNPs presented no inhibitory effect on A549 cell invasion however TK-AuNPs also showed a slight anti-adhesive effect to fibronectin (~20% inhibition) and insignificant inhibition on MMP-2 production (~30% inhibition) of A549 cells.

Conclusively, fucoidans from two species of marine brown algae; *C. okamuranus* and *K. crassifolia* have an ability to synthesize AuNPs with simple and eco-friendly method. Moreover, the fucoidan-stabilized AuNPs might be a promising compound for cancer therapy as well as the prevention of cancer metastasis. In the future, fucoidan-stabilized AuNPs should be further investigated on anti-tumor mechanisms of the AuNPs and *in vivo* study to find out whether the AuNPs could be applied in the real situation.

REFERENCES

Aisa, Y., Miyakawa, Y., Nakazato, T., Shibata, H., Saito, K., Ikeda, Y., and Kizaki, M. 2005. Fucoidan induces apoptosis of human HS-Sultan cells accompanied by activation of caspase-3 and down-regulation of ERK pathways. Am. J. Hematol. 78(1): 7-14.

Alkilany, A. M., Nagaria, P. K., Wyatt, M. D., and Murphy, C. J. 2010. Cation exchange on the surface of gold nanorods with a polymerizable surfactant: polymerization, stability, and toxicity evaluation. Langmuir 26(12): 9328-9333.

Alley, M. C., Scudiero, D. A., Monks, A., Hursey, M. L., Czerwinski, M. J., Fine, D. L., Abbott, B. J., Mayo, J. G., Shoemaker, R. H., and Boyd, M. R. 1988. Feasibility of drug screening with panels of human tumor cell lines using a microculture tetrazolium assay. Cancer Res. 48(3): 589-601.

Asadishad, B., Vossoughi, M., and Alamzadeh, I. 2010. *In vitro* release behavior and cytotoxicity of doxorubicin-loaded gold nanoparticles in cancerous cells. Biotechnol. Lett. 32(5): 649-654.

Berteau, O., and Mulloy, B. 2003. Sulfated fucans, fresh perspectives: Structures, functions, and biological properties of sulfated fucans and an overview of enzymes active toward this class of polysaccharide. Glycobiology 13(6): 29R-40R.

Bhainsa, K. C., and D'Souza, S. F. 2006. Extracellular biosynthesis of silver nanoparticles using the fungus *Aspergillus fumigatus*. Colloids Surf. B Biointerfaces 47(2): 160-164.

Bhattacharya, R., and Mukherjee, P. 2008. Biological properties of "Naked" Metal nanoparticles. Adv. Drug Deliv. Rev. 60(11): 1289-1306.

Bhumkar, D. R., Joshi, H. M., Sastry, M., and Pokharkar, V. B. 2007. Chitosan reduced gold nanoparticles as novel carriers for transmucosal delivery of insulin. Pharm. Res. 24(8): 1415-1426.

Brooks, S. A., Lomax-Browne, H. J., Carter, T. M., Kinch, C. E., and Hall, D. M. S. 2008. Molecular interactions in cancer cell metastasis. Acta. Histochemica. 112(1): 3-25.

Brunner, G., Reimbold, K., Meissauer, A., Schirrmacher, V., and Erkell, L. J. 1998. Sulfated glycosaminoglycans enhance tumor cell invasion *in vitro* by stimulating plasminogen activation. Exp. Cell Res. 239(2): 301-310.

Byrne, J. D., Betancourt, T., and Brannon-Peppas, L. 2008. Active targeting schemes for nanoparticle systems in cancer therapeutics. Adv. Drug Deliv. Rev. 60(15): 1615-1626.

Chen, P. C., Mwakwari, S. C., and Oyelere, A. K. 2008. Gold nanoparticles: From nanomedicine to nanosensing. Nanotechnol. Sci. Appl. 2008: 45-66.

Cumashi, A., Ushakova, N. A., Preobrazhenskaya, M. E., D'Incecco, A., Piccoli, A., Totani, L., Tinari, N., Morozevich, G. E., Berman, A. E., Bilan, M. I., Usov, A. I., Ustyuzhanina, N. E., Grachev, A. A., Sanderson, C. J., Kelly, M., Rabinovich, G. A., Iacobelli, S., and Nifantiev, N. E. 2007. A comparative study of the anti-inflammatory, anticoagulant, antiangiogenic, and antiadhesive activities of nine different fucoidans from brown seaweeds. Glycobiology 17(5): 541-552.

De Azevedo, T. C., Bezerra, M. E., Santos Mda, G., Souza, L. A., Marques, C. T., Benevides, N. M., and Leite, E. L. 2009. Heparinoids algal and their anticoagulant, hemorrhagic activities and platelet aggregation. Biomed. Pharmacother. 63(7): 477-483.

Dingler, A., Blum, R. P., Niehus, H., Muller, R. H., and Gohla, S. 1999. Solid lipid nanoparticles (SLN/Lipopearls)--a pharmaceutical and cosmetic carrier for the application of vitamin e in dermal products. J. Microencapsul. 16(6): 751-767.

Dreaden, E. C., Mwakwari, S. C., Sodji, Q. H., Oyelere, A. K., and El-Sayed, M. A. 2009. Tamoxifen-poly(ethylene glycol)-thiol gold nanoparticle conjugates: enhanced potency and selective delivery for breast cancer treatment. Bioconjug. Chem. 20(12): 2247-2253.

El-Sayed, I. H., Huang, X., and El-Sayed, M. A. 2006. Selective laser photo-thermal therapy of epithelial carcinoma using anti-EGFR antibody conjugated gold nanoparticles. Cancer Lett. 239(1): 129-135.

Fitton, J. H., Irhimeh, M., and Falk, N. 2007. Macroalgal fucoidan extracts: A new opportunity for marine cosmetics. Cosmetics and Toiletries 122(8): 55-64.

Frankel, A., Buckman, R., and Kerbel, R. S. 1997. Abrogation of taxol-induced G2-M arrest and apoptosis in human ovarian cancer cells grown as multicellular tumor spheroids. Cancer Res. 57(12): 2388-2393.

Fukahori, S., Yano, H., Akiba, J., Ogasawara, S., Momosaki, S., Sanada, S., Kuratomi, K., Ishizaki, Y., Moriya, F., Yagi, M., and Kojiro, M. 2008. Fucoidan, a major component of brown seaweed, prohibits the growth of human cancer cell lines *in vitro*. Mol. Med. Reports 1(4): 537-542.

Fukazawa, H.,Mizuno, S., and Uehara, Y. 1995. A microplate assay for quantitation of anchorage-independent growth of transformed cells. Anal. Biochem. 228(1): 83-90.

Ghosh, P., Han, G., De, M., Kim, C. K., and Rotello, V. M. 2008. Gold nanoparticles in delivery applications. Adv. Drug Deliv. Rev. 60(11): 1307-1315.

Gibson, J. D., Khanal, B. P., and Zubarev, E. R. 2007. Paclitaxel-functionalized gold nanoparticles. J. Am. Chem. Soc. 129(37): 11653-11661.

Gideon, T. P., and Rengasamy, R. 2008. Toxicological evaluation of fucoidan from *Cladosiphon okamuranus*. J. Med. Food 11(4): 638-642.

Giraux, J. L., Matou, S., Bros, A., Tapon-Bretaudiere, J., Letourneur, D., and Fischer, A. M. 1998. Modulation of human endothelial cell proliferation and migration by fucoidan and heparin. Eur. J. Cell Biol. 77(4): 352-359.

Haneji, K., Matsuda, T., Tomita, M., Kawakami, H., Ohshiro, K., Uchihara, J. N., Masuda, M., Takasu, N., Tanaka, Y., Ohta, T., and Mori, N. 2005. Fucoidan extracted from *Cladosiphon okamuranus* tokida induces apoptosis of human T-cell leukemia virus type 1-infected T-cell lines and primary adult T-cell leukemia cells. Nutr. Cancer 52(2): 189-201.

Hayashi, K., Nakano, T., Hashimoto, M., Kanekiyo, K., and Hayashi, T. 2008. Defensive effects of a fucoidan from brown alga *Undaria pinnatifida* against herpes simplex virus infection. Int. Immunopharmacol. 8(1): 109-116.

Hornig, S., Bunjes, H., and Heinze, T. 2009. Preparation and characterization of nanoparticles based on dextran-drug conjugates. J. Colloid Interface Sci. 338(1): 56-62.

Hosta, L., Pla-Roca, M., Arbiol, J., Lopez-Iglesias, C., Samitier, J., Cruz, L. J., Kogan, M. J., and Albericio, F. 2009. Conjugation of kahalalide F with gold nanoparticles to enhance *in vitro* antitumoral activity. Bioconjug. Chem. 20(1): 138-146.

Huang, H., and Yang, X. 2004. Synthesis of polysaccharide-stabilized gold and silver nanoparticles: A green method. Carbohydr. Res. 339(15): 2627-2631.

Huang, S.-H. 2007. Gold nanoparticle-based immunochromatographic assay for the detection of *Staphylococcus aureus*. Clin. Chim. Acta. 127(2): 335-340.

Hyun, J. H., Kim, S. C., Kang, J. I., Kim, M. K., Boo, H. J., Kwon, J. M., Koh, Y. S., Hyun, J. W., Park, D. B., Yoo, E. S., and Kang, H. K. 2009. Apoptosis inducing activity of fucoidan in HCT-15 colon carcinoma cells. Biol. Pharm. Bull. 32(10): 1760-1764.

Jain, P. K., El-Sayed, I. H., and El-Sayed, M. A. 2007. Au nanopartices target cancer. Nano Today 2(2): 18-29.

Jemal, A., Siegel, R., Ward, E., Hao, Y., Xu, J., Murray, T., and Thun, M. J. 2008. Cancer statistics, 2008. CA. Cancer J. Clin. 58(2): 71-96.

Jiang, Z., Okimura, T., Yokose, T., Yamasaki, Y., Yamaguchi, K., and Oda, T. 2010. Effects of sulfated fucan, ascophyllan, from the brown alga *Ascophyllum nodosum* on various cell lines: A comparative study on ascophyllan and fucoidan. J. Biosci. Bioeng. 110(1): 113-117.

Jiao, Q., and Liu, Q. 1999. Simple spectrophotometric method for the estimation of algal polysaccharide concentrations. J. Agric. Food Chem. 47(3): 996-998.

Karmakar, P., Pujol, C. A., Damonte, E. B., Ghosh, T., and Ray, B. 2010. Polysaccharides from *Padina tetrastromatica*: Structural features, chemical modification and antiviral activity. Carbohydr. Polym. 80(2): 513-520.

Kikkawa, Y., Sanzen, N., and Sekiguchi, K. 1998. Isolation and characterization of laminin-10/11 secreted by human lung carcinoma cells. Laminin-10/11 mediates cell adhesion through integrin alpha3 beta1. J. Biol. Chem. 273(25): 15854-15859.

Kim, K. J., Lee, O. H., Lee, H. H., and Lee, B. Y. 2009. A 4-week repeated oral dose toxicity study of fucoidan from the sporophyll of *Undaria pinnatifida* in Sprague-Dawley rats. Toxicology 267(1-3): 154-158.

Kimling, J.;Maier, M.;Okenve, B.;Kotaidis, V.;Ballot, H.; and Plech, A. 2006. Turkevich method for gold nanoparticle synthesis revisited. J. Phys. Chem. B 110(32): 15700-15707.

Krishnamachary, B., Berg-Dixon, S., Kelly, B., Agani, F., Feldser, D., Ferreira, G., Iyer, N., LaRusch, J., Pak, B., Taghavi, P., and Semenza, G. L. 2003. Regulation of colon carcinoma cell invasion by hypoxia-inducible factor 1. Cancer Res. 63(5): 1138-1143.

Lake, A. C., Vassy, R., Di Benedetto, M., Lavigne, D., Le Visage, C., Perret, G. Y., and Letourneur, D. 2006. Low molecular weight fucoidan increases VEGF165-induced endothelial cell migration by enhancing VEGF165 binding to VEGFR-2 and NRP1. J. Biol. Chem. 281(49): 37844-37852.

Lee, N. Y., Ermakova, S. P., Zvyagintseva, T. N., Kang, K. W., Dong, Z., and Choi, H. S. 2008. Inhibitory effects of fucoidan on activation of epidermal growth factor

receptor and cell transformation in JB6 CL41 cells. Food Chem. Toxicol. 46(5): 1793-1800.

Lee, S. J., Sakurai, H., Oshima, K., Kim, S. H., and Saiki, I. 2003. Anti-metastatic and anti-angiogenic activities of a new matrix metalloproteinase inhibitor, TN-6b. Eur. J. Cancer 39(11): 1632-1641.

Lewinski, N., Colvin, V., and Drezek, R. 2008. Cytotoxicity of nanoparticles. Small 4(1): 26-49.

Li, B., Lu, F., Wei, X., and Zhao, R. 2008. Fucoidan: Structure and bioactivity. Molecules 13(8): 1671-1695.

Li, J. L., Wang, L., Liu, X. Y., Zhang, Z. P., Guo, H. C., Liu, W. M., and Tang, S. H. 2009. *In vitro* cancer cell imaging and therapy using transferrin-conjugated gold nanoparticles. Cancer Lett. 274(2): 319-326.

Likhatskii, M. N., and Mikhlin, Y. L. 2007. Influence of sulfide ions on the formation and properties of gold nanoparticles in aqueous solutions. Glass Physics and Chemistry 33(4): 422-425.

Link, S., and El-sayed, M. A. 1999. Spectral properties and relaxation dynamics of surface plasmon electronic oscillations in gold and silver nanodots and nanorods. J. Phys. Chem. B 103(40): 8410–8426

Lirdprapamongkol, K., Sakurai, H., Kawasaki, N., Choo, M. K., Saitoh, Y., Aozuka, Y., Singhirunnusorn, P., Ruchirawat, S., Svasti, J., and Saiki, I. 2005. Vanillin suppresses *in vitro* invasion and *in vivo* metastasis of mouse breast cancer cells. Eur. J. Pharm. Sci. 25(1): 57-65.

Liu, J. M., Bignon, J., Haroun-Bouhedja, F., Bittoun, P., Vassy, J., Fermandjian, S., Wdzieczak-Bakala, J., and Boisson-Vidal, C. 2005. Inhibitory effect of fucoidan on the adhesion of adenocarcinoma cells to fibronectin. Anticancer Res. 25(3B): 2129-2133.

Matsumoto, S., Nagaoka, M., Hara, T., Kimura-Takagi, I., Mistuyama, K., and Ueyama, S. 2004. Fucoidan derived from *Cladosiphon okamuranus* tokida ameliorates murine chronic colitis through the down-regulation of interleukin-6 production on colonic epithelial cells. Clin. Exp. Immunol. 136(3): 432-439.

Mukherjee, P., Bhattacharya, R., Wang, P., Wang, L., Basu, S., Nagy, J. A., Atala, A., Mukhopadhyay, D., and Soker, S. 2005. Antiangiogenic properties of gold nanoparticles. Clin. Cancer Res. 11(9): 3530-3534.

Mukherjee, P., Bhattacharya, R., Bone, N., Lee, Y. K., Patra, C. R., Wang, S., Lu, L., Secreto, C., Banerjee, P. C., Yaszemski, M. J., Kay, N. E., and Mukhopadhyay, D. 2007. Potential therapeutic application of gold nanoparticles in b-chronic lymphocytic leukemia (BCLL): Enhancing apoptosis. J Nanobiotechnology 5: 4.

Nath, S., Kaittanis, C., Tinkham, A., and Perez, J. M. 2008. Dextran-coated gold nanoparticles for the assessment of antimicrobial susceptibility. Anal. Chem. 80(4): 1033-1038.

O'Neill, A. N. 1954. Degradative studies on fucoidan. J. Amer. Chem. Soc. 76: 5074-5076

Park, C., Youn, H., Kim, H., Noh, T., Kook, Y. H., Oh, E. T., Park, H. J., and Kim, C. 2009. Cyclodextrin-covered gold nanoparticles for targeted delivery of an anti-cancer drug. J. Mater. Chem. 19: 2310–2315

Patankar, M. S., Oehninger, S., Barnett, T., Williams, R. L., and Clark, G. F. 1993. A revised structure for fucoidan may explain some of its biological activities. J. Biol. Chem. 268(29): 21770-21776.

Patra, C. R., Bhattacharya, R., and Mukherjee, P. 2009. Fabrication and functional characterization of goldnanoconjugates for potential application in ovarian cancer. J. Mater. Chem. 20: 547-554.

Polte, J., Ahner, T. T., Delissen, F., Sokolov, S., Emmerling, F., Thunemann, A. F., and Kraehnert, R. 2010. Mechanism of gold nanoparticle formation in the classical citrate synthesis method derived from coupled *in situ* XANES and SAXS evaluation. J. Am. Chem. Soc. 132(4): 1296-1301.

Qu, Y., and Lu, X. 2009. Aqueous synthesis of gold nanoparticles and their cytotoxicity in human dermal fibroblasts-fetal. Biomed. Mater. 4(2): 025007.

Rahman, M., Abd-El-Barr, M., Vivian Macka, T. T., Sokolov, K., Richards-Kortum, R., and Descour, M. 2005. Optical imaging of cervical pre-cancers with structured illumination: An integrated approach. Gynecologic. Oncology 99: S112 – S115.

Rocha, H. A., Franco, C. R., Trindade, E. S., Carvalho, L. C., Veiga, S. S., Leite, E. L., Dietrich, C. P., and Nader, H. B. 2001. A fucan from the brown seaweed *Spatoglossum schroederi* inhibits chinese hamster ovary cell adhesion to several extracellular matrix proteins. Braz. J. Med. Biol. Res. 34(5): 621-626.

Rocha, H. A., Franco, C. R., Trindade, E. S., Veiga, S. S., Leite, E. L., Nader, H. B., and Dietrich, C. P. 2005. Fucan inhibits Chinese hamster ovary cell (CHO) adhesion to fibronectin by binding to the extracellular matrix. Planta. Med. 71(7): 628-633.

Sakai, T., Ishizuka, K., Shimanaka, K., Ikai, K., and Kato, I. 2003. Structures of oligosaccharides derived from *Cladosiphon okamuranus* fucoidan by digestion with marine bacterial enzymes. Mar. Biotechnol. (N.Y.) 5(6): 536-544.

Sanvicens, N., and Marco, M. P. 2008. Multifunctional nanoparticles--properties and prospects for their use in human medicine. Trends Biotechnol. 26(8): 425-433.

Semenza, G. L. 2003. Targeting HIF-1 for cancer therapy. Nat. Rev. Cancer 3(10): 721-732.

Shibata, H., Iimuro, M., Uchiya, N., Kawamori, T., Nagaoka, M., Ueyama, S., Hashimoto, S., Yokokura, T., Sugimura, T., and Wakabayashi, K. 2003. Preventive effects of Cladosiphon fucoidan against *Helicobacter pylori* infection in *Mongolian gerbils*. Helicobacter. 8(1): 59-65.

Simpson, C. D., Anyiwe, K., and Schimmer, A. D. 2008. Anoikis resistance and tumor metastasis. Cancer Lett. 272(2): 177-185.

Singaravelu, G., Arockiamary, J. S., Kumar, V. G., and Govindaraju, K. 2007. A novel extracellular synthesis of monodisperse gold nanoparticles using marine alga, *Sargassum wightii* Greville. Colloids Surf. B Biointerfaces 57(1): 97-101.

Singh, R., and Lillard, J. W., Jr. 2009. Nanoparticle-based targeted drug delivery. Exp. Mol. Pathol. 86(3): 215-223.

Sinha, S., Astani, A., Ghosh, T., Schnitzler, P., and Ray, B. 2010. Polysaccharides from *Sargassum tenerrimum*: Structural features, chemical modification and anti-viral activity. Phytochemistry 71(2-3): 235-242.

Soeda, S.;Ishida, S.;Shimeno, H.; and Nagamatsu, A. 1944. Inhibitory effect of oversulfated fucoidan on invasion through reconstituted basement membrane by murine Lewis lung carcinoma. Jpn. J. Cancer Res. 85(11): 1144-1150.

Stoker, M., Gherardi, E., Perryman, M., and Gray, J. 1987. Scatter factor is a fibroblast-derived modulator of epithelial cell mobility. Nature 327(6119): 239-242.

Sun, C., Qu, R., Chen, H., Ji, C., Wang, C., Sun, Y., and Wang, B. 2008. Degradation behavior of chitosan chains in the 'green' synthesis of gold nanoparticles. Carbohydr. Res. 343(15): 2595-2599.

Synytsya, A., Kim, W. J., Kim, S. M., Pohl, R., Synytsya, A., Kvasnicka, F., Copikova, J., and Park, Y. I. 2010. Structure and antitumour activity of fucoidan isolated from Sporophyll of Korean brown seaweed *Undaria pinnatifida.* Carbohydr. Polym. 81(1): 41-48.

Takara Bio Inc. Takara Kombu fucoidan [online]. (n.d.). Available from: www.takara-bio.com/products/pdfs/fuco.pdf [2009, February 19]

Teruya, T., Konishi, T., Uechi, S., Tamaki, H., and Tako, M. 2007. Anti-proliferative activity of oversulfated fucoidan from commercially cultured *Cladosiphon okamuranus* tokida in U937 cells. Int. J. Biol. Macromol. 41(3): 221-226.

Wang, L. H. 2004. Molecular signaling regulating anchorage-independent growth of cancer cells. Mt. Sinai. J. Med. 71(6): 361-367.

Winter, J. Gold nanoparticle biosensors [Online]. 2007. Available from: http://www.nsec.ohio-state.edu/teacher_workshop/Gold_Nanoparticles.pdf [2009, June 22]

World Health Organization (WHO). Cancer [online]. (2009). Available from: http://www.who.int/mediacentre/factsheets/fs297/en/ [2010, June 30]

Xi, D., Luo, X., Ning, Q., Lu, Q., Yao, K., and Liu, Z. 2007. The detection of HBV DNA with gold nanoparticle gene probes. J. Nanjing Med. Univ. 21(4): 207-212.

Yang, J. W., Yoon, S. Y., Oh, S. J., Kim, S. K., and Kang, K. W. 2006. Bifunctional effects of fucoidan on the expression of inducible nitric oxide synthase. Biochem. Biophys. Res. Commun. 346(1): 345-350.

Ye, J., Li, Y., Teruya, K., Katakura, Y., Ichikawa, A., Eto, H., Hosoi, M., Nishimoto, S., and Shirahata, S. 2005. Enzyme-digested fucoidan extracts derived from seaweed mozuku of *Cladosiphon novae-caledoniae kylin* inhibit invasion and angiogenesis of tumor cells. Cytotechnology 47(1-3): 117-126.

Zhang, Z., Han, L., Cao, L., Liang, X., Liu, Y., Liu, H., Du, J., Qu, Z., Zhu, C., Liu, S., Li, H., and Sun, W. 2008. Aggregation formation mediated anoikis resistance of BEL7402 hepatoma cells. Folia. Histochem. Cytobiol. 46(3): 331-336.

APPENDICES

Appendix A: X-ray energy dispersive spectroscopy (EDS) pattern of fucodian-stabilized AuNPs

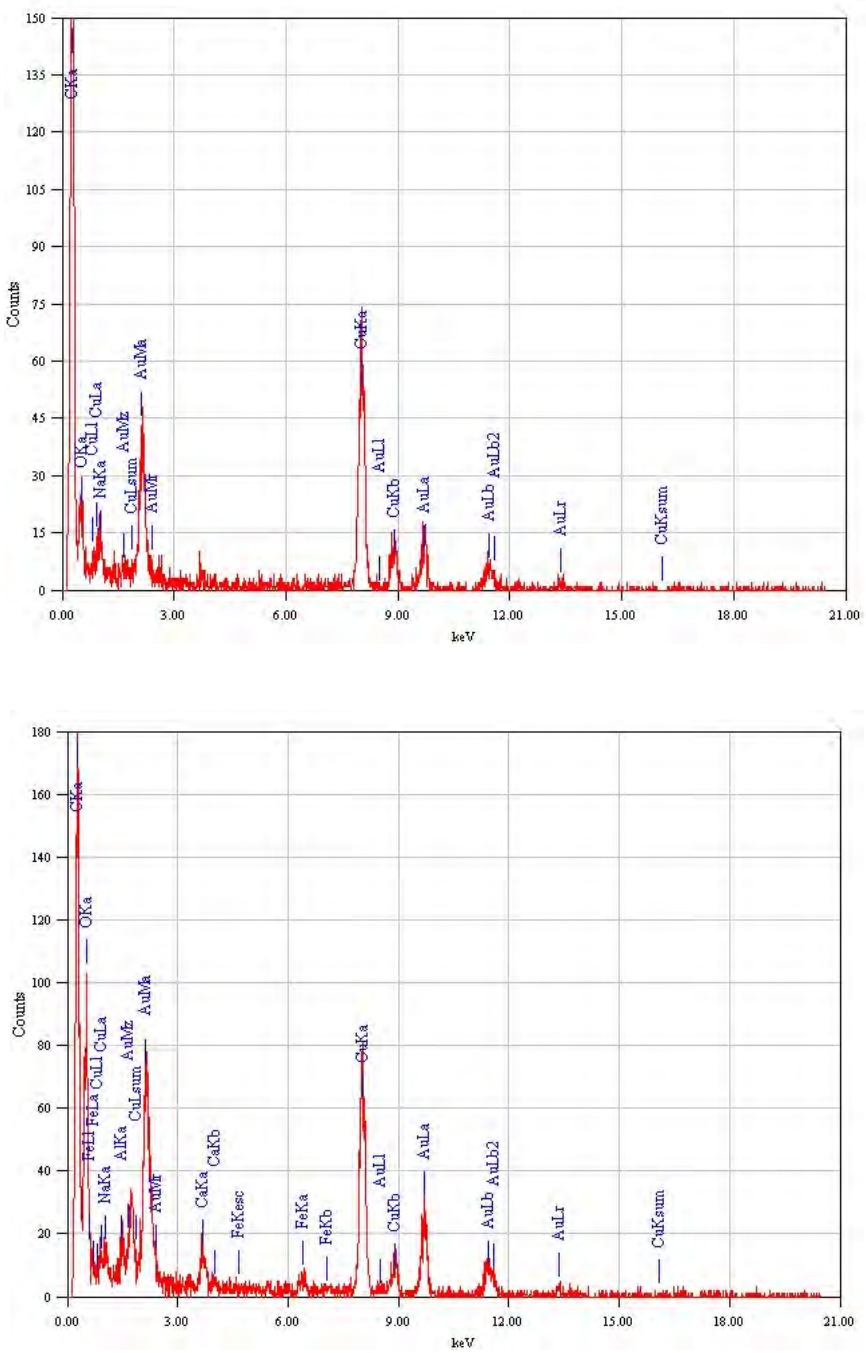

Figure A1 EDS pattern of OM-AuNPs (top) and TK-AuNPs (bottom)

Appendix B: Estimation of fucoidan amount in the colloidal gold nanoparticles

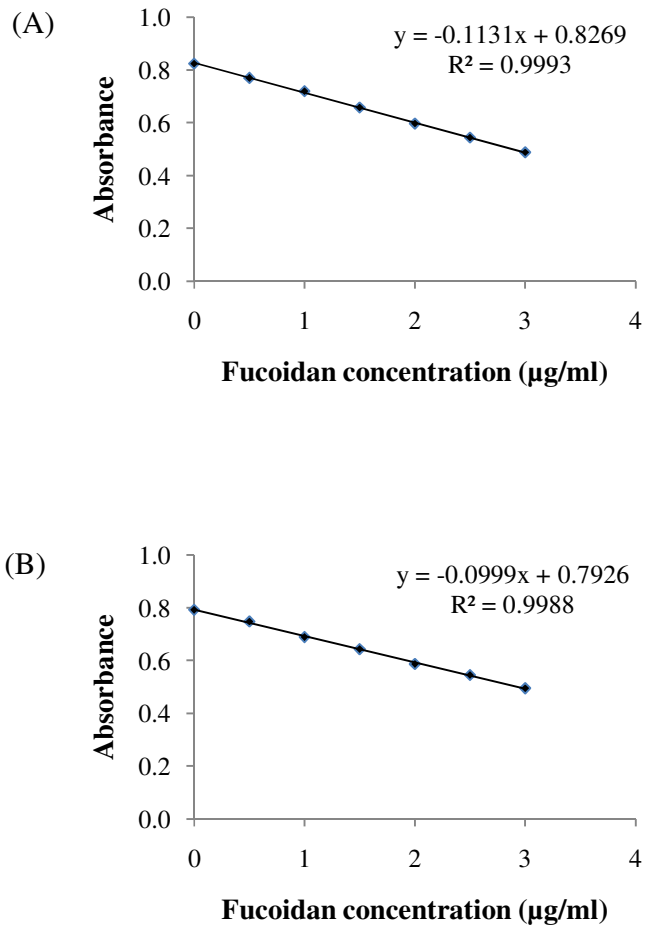

Figure B1 Examples of calibration curve between UV-absorbance and concentration of OM fucoidan (A) and TK fucoidan (B)

Table B1 Average concentration of OM fucoidan in the colloidal gold nanoparticles

Sample No.	1	2	3	Average concentration ± S.D. (n=3)
1	3.19	2.72	2.64	2.85 ± 0.30
2	2.05	2.64	2.45	2.38 ± 0.30
3	2.92	3.38	3.32	3.21 ± 0.25

Table B2 Average concentration of TK fucoidan in the colloidal gold nanoparticles

Sample No.	1	2	3	Average concentration ± S.D. (n=3)
1	5.87	6.33	6.28	6.16 ± 0.25
2	7.20	8.17	6.90	7.42 ± 0.66
3	6.39	6.13	6.44	6.32 ± 0.17

Table B3 Fucoidan concentration in fucoidan-stabilized AuNPs colloid

Type of stabilizer	Concentration (mg/ml)			Average concentration (mg/ml) ± S.D. (n=3)
	1	2	3	
OM fucoidan	2.85	2.38	3.21	2.81 ± 0.42
TK fucoidan	6.16	7.42	6.32	6.63 ± 0.69

Appendix C: A549 cell viability after treatment with samples in anchorage-dependent condition

Table C1 Percentage of viability of A549 cells after treatment with OM fucoidan and OM-AuNPs for 24 and 72 hours (Average ± S.D., n=3)

Duration of treatment (hrs)	Samples	Dose (µg/ml)	Viability (%)				
			Exp 1	Exp 2	Exp 3	Average	S.D.
24	OM fucoidan	30	89.67	87.28	77.63	84.86	6.37
		100	76.40	76.97	66.59	73.32	5.84
		300	82.04	81.25	68.83	77.38	7.41
	OM-AuNPs	30	68.99	65.24	61.89	65.37*	3.55
		100	75.00	61.63	55.67	64.10	9.90
		300	60.82	59.52	54.01	58.11*	3.62
72	OM fucoidan	30	81.28	81.30	80.57	81.05	0.42
		100	70.91	75.86	68.87	71.88	3.60
		300	66.14	70.39	67.01	67.84	2.24
	OM-AuNPs	30	70.41	70.96	72.94	71.44*	1.33
		100	55.25	62.06	59.02	58.78*	3.41
		300	44.64	46.23	48.16	46.35*	1.76

Table C2 Percentage of viability of A549 cells after treatment with TK fucoidan and TK-AuNPs for 24 and 72 hours (Average ± S.D., n=3)

Duration of treatment (hrs)	Samples	Dose (µg/ml)	Viability (%)				
			Exp 1	Exp 2	Exp 3	Average	S.D.
24	TK fucoidan	30	74.38	75.39	70.62	73.46	2.51
		100	74.24	68.95	66.80	70.00	3.83
		300	68.32	66.22	64.77	66.44	1.79
	TK-AuNPs	30	74.38	75.39	70.62	73.46*	2.51
		100	74.24	68.95	66.80	70.00*	3.83
		300	68.32	66.22	64.77	66.44*	1.79
72	TK fucoidan	30	73.51	80.22	78.53	77.42	3.49
		100	68.71	72.89	75.58	72.39	3.46
		300	67.21	70.38	69.54	69.04	1.64
	TK-AuNPs	30	73.51	80.22	78.53	77.42*	3.49
		100	68.71	72.89	75.58	72.39*	3.46
		300	67.21	70.38	69.54	69.04*	1.64

* are significant differences at $p \leq 0.05$ of AuNPs compared to solely fucoidan.

Table C3 Percentage of viability of A549 cells after treatment with Cit-AuNPs for 24 and 72 hours (Average ± S.D., n=3)

Duration of treatment (hrs)	**Dose (μM)**	**Viability (%)**				
		Exp 1	**Exp 2**	**Exp 3**	**Average**	**S.D.**
24	91	101.82	101.57	94.74	99.38	4.02
	215	100.53	101.01	92.28	97.94	4.91
72	91	99.73	104.29	104.22	102.71	2.60
	215	95.14	96.24	100.73	97.37	3.00

Appendix D: A549 cell viability after treatment with samples in anchorage-independent condition

Table D1 Percentage of viability of A549 cells after treatment with OM fucoidan and OM-AuNPs for 24 and 72 hours (Average ± S.D., n=3)

Duration of treatment (hrs)	Samples	Dose (µg/ml)	Viability (%)				
			Exp 1	Exp 2	Exp 3	Average	S.D.
24	OM fucoidan	30	108.03	90.14	94.30	97.49	9.36
		100	105.15	85.85	81.22	90.74	12.69
		300	98.75	76.48	75.87	83.70	13.04
	OM-AuNPs	30	85.23	77.24	84.95	82.47	4.53
		100	76.76	78.38	82.49	79.21	2.95
		300	75.90	57.04	80.00	70.98	12.24
72	OM fucoidan	30	85.24	92.02	78.91	85.39	6.55
		100	84.93	83.22	69.52	79.22	8.45
		300	64.58	59.85	53.34	59.26	5.64
	OM-AuNPs	30	81.58	83.78	90.77	85.38	4.80
		100	77.59	69.85	84.94	77.46	7.55
		300	64.12	42.10	59.08	55.10	11.54

Table D2 Percentage of viability of A549 cells after treatment with TK fucoidan and TK-AuNPs for 24 and 72 hours (Average ± S.D., n=3)

Duration of treatment (hrs)	Samples	Dose (µg/ml)	Viability (%)				
			Exp 1	Exp 2	Exp 3	Average	S.D.
24	TK fucoidan	30	108.92	92.10	102.05	101.02	8.46
		100	93.84	85.74	87.97	89.18	4.18
		300	89.16	79.12	78.94	82.41	5.85
	TK-AuNPs	30	86.72	80.12	80.96	82.60	3.59
		100	77.29	69.21	84.69	77.06	7.74
		300	81.15	85.29	83.37	83.27	2.07
72	TK fucoidan	30	93.65	96.39	92.08	94.04	2.18
		100	71.11	74.50	68.26	71.29	3.12
		300	67.90	63.67	65.85	65.81	2.11
	TK-AuNPs	30	81.13	77.02	89.49	82.54	6.36
		100	74.80	71.62	88.19	78.20	8.79
		300	73.58	60.02	72.79	68.80	7.61

Table D3 Percentage of viability of A549 cells after treatment with Cit-AuNPs for 24 and 72 hours (Average ± S.D., n=3)

Duration of treatment (hrs)	**Dose (μM)**	**Viability (%)**				
		Exp 1	**Exp 2**	**Exp 3**	**Average**	**S.D.**
24	91	116.18	100.41	95.45	104.01	10.83
	215	107.21	88.16	87.94	94.44	11.06
72	91	98.81	112.96	105.02	105.60	7.09
	215	98.30	97.83	81.96	92.70	9.30

Appendix E: Photographs of A549 cells after incubation in regular or poly-HEMA coated 96-well plate

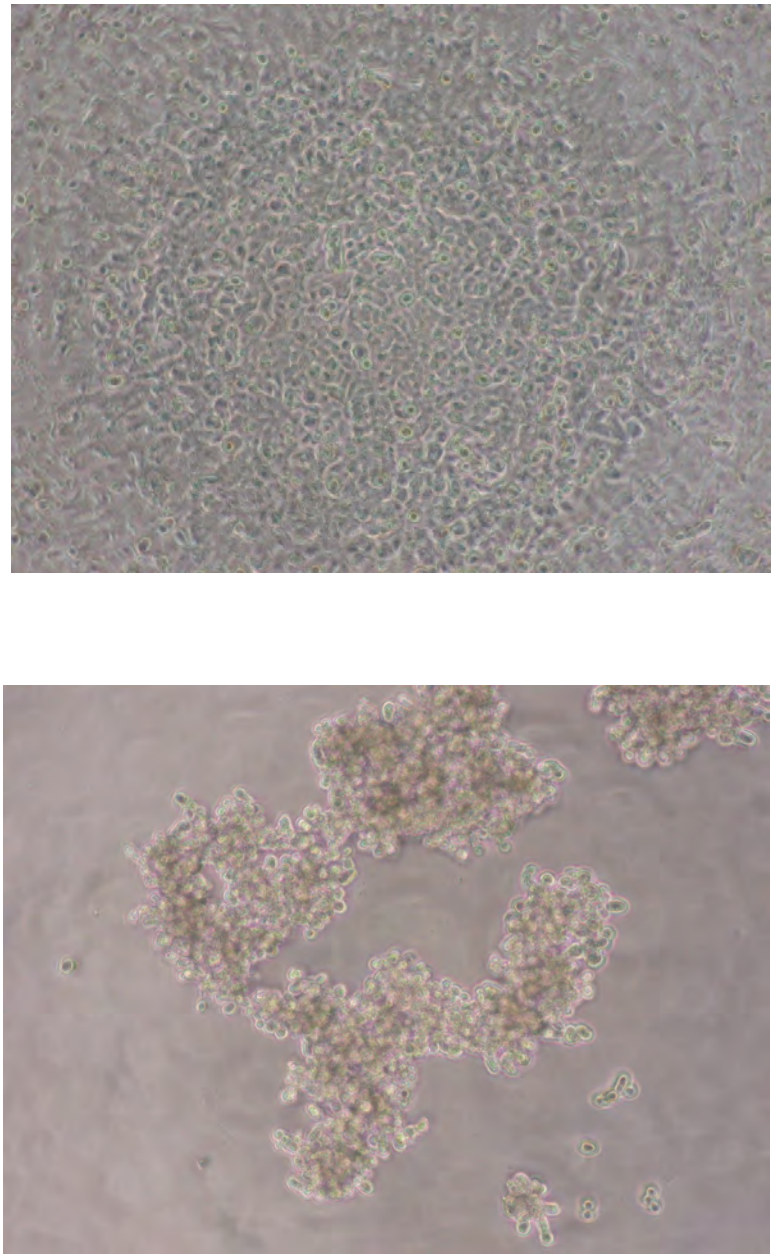

Figure E1 Photographs (original magnification was x100) of A549 cells after incubation in regular 96-well plate (top) and poly-HEMA 96-well plate (bottom)

Appendix F: A549 cell invasion and cell migration after 6-hour treatment with samples

Table F1 Percentage of invasion of A549 cells after treatment of 300 µg/ml fucoidans, fucoidan-stabilized AuNPs containing 300 µg/ml fucoidans and 215 µM Cit-AuNPs (Average ± S.D., n=3)

Samples	Invasion (%)				
	Exp 1	Exp 2	Exp 3	Average	S.D.
OM fucoidan	87.18	90.92	87.83	88.64*	2.00
OM-AuNPs	86.19	80.14	88.13	84.82*	4.17
TK fucoidan	115.34	81.80	97.93	98.36	16.77
TK-AuNPs	131.38	126.46	86.38	114.74	24.69
Cit-AuNPs	95.75	79.79	82.41	85.99*	8.56

* are significant differences at $p \leq 0.05$ compared to a control (medium).

Table F2 Percentage of cell migration of A549 cells after treatment of 300 µg/ml fucoidans, fucoidan-stabilized AuNPs containing 300 µg/ml fucoidans and 215 µM Cit-AuNPs (Average ± S.D., n=3)

Samples	Cell migration (%)				
	Exp 1	Exp 2	Exp 3	Average	S.D.
OM fucoidan	158.57	84.57	152.48	131.87	41.08
OM-AuNPs	117.87	78.62	135.50	110.66	29.12
TK fucoidan	163.56	80.56	177.64	140.58	52.46
TK-AuNPs	111.39	84.78	203.29	133.15	62.18
Cit-AuNPs	138.35	68.29	109.28	105.31	35.20

Appendix G: A549 cell adhesion after 1-hour treatment with samples

Table G1 Percentage of adhesion of A549 cells to Matrigel® after treatment of 300 µg/ml fucoidans, fucoidan-stabilized AuNPs containing 300 µg/ml fucoidans and 215 µM Cit-AuNPs (Average ± S.D., n=3)

Samples	Cell adhesion (%)				
	Exp 1	**Exp 2**	**Exp 3**	**Average**	**S.D.**
OM fucoidan	146.56	146.56	97.70	130.27	28.21
OM-AuNPs	143.43	143.43	149.02	145.29	3.23
TK fucoidan	94.15	93.46	94.39	94.00	0.48
TK-AuNPs	87.84	93.39	85.01	88.75	4.26
Cit-AuNPs	105.54	105.54	96.63	102.57	5.15

Table G2 Percentage of adhesion of A549 cells to fibronectin after treatment of 300 µg/ml fucoidans, fucoidan-stabilized AuNPs containing 300 µg/ml fucoidans and 215 µM Cit-AuNPs (Average ± S.D., n=3)

Samples	Cell adhesion (%)				
	Exp 1	**Exp 2**	**Exp 3**	**Average**	**S.D.**
OM fucoidan	73.20	98.59	72.78	81.52	14.78
OM-AuNPs	88.67	62.46	69.26	73.46*	13.60
TK fucoidan	90.72	86.64	95.06	90.81*	4.21
TK-AuNPs	79.69	76.09	87.35	81.04*	5.75
Cit-AuNPs	99.12	94.15	103.63	98.97	4.74

* are significant differences at $p \leq 0.05$ compared to a control (medium).

Appendix H: MMP-2 production of A549 cells after 24-hour treatment with samples

Table H1 Percentage of MMP-2 production of A549 cells after treatment of 300 µg/ml fucoidans, fucoidan-stabilized AuNPs containing 300 µg/ml fucoidans and 215 µM Cit-AuNPs (Average ± S.D., n=3)

Samples	**MMP-2 production (%)**				
	Exp 1	**Exp 2**	**Exp 3**	**Average**	**S.D.**
OM fucoidan	34.93	47.50	77.15	53.19*	21.68
OM-AuNPs	41.37	27.13	62.78	43.76*	17.95
TK fucoidan	107.23	80.44	97.31	94.99	13.54
TK-AuNPs	98.79	29.26	87.35	71.80	37.28
Cit-AuNPs	65.76	61.04	135.45	87.42	41.66

* are significant differences at $p \leq 0.05$ compared to a control (medium).

VITA

Miss Suwicha Soisuwan was born on April 23, 1985 in Bangkok, Thailand. She received the Bechelor Degree of Pharmacy (the first class honour) from Srinakharinwirot University in 2008. After that, she gained admission to Graduate School of Chulalongkorn University in the Faculty of Pharmaceutical science in Pharmaceutical Technology (International Program).

Publications:

Soisuwan, S., Warisnoicharoen, W., Lirdprapamongkol, K., and Svasti, J. 2010. Eco-friendly synthesis of fucoidan-stabilized gold nanoparticles. Am. J. Applied Sci. 7(8): 1038-1042.

Soisuwan, S., Mapaisansin, W., Samee, W., Brantner, A.H., and Kamkaen, N. 2010. Development of peacock flower extract as anti-wrinkle formulation. J. Health Res. 24(1): 29-34.